FORUM GEOGRAFI
ISSN: 0852-0682 | E-ISSN: 2460-3945

HTTPS://JOURNALS.UMS.AC.ID/INDEX.PHP/FG/

Research article

Assessing Household Climate Resilience Index to Climate Change Impacts in DKI Jakarta: A Robust Geographically Weighted PCA Approach

Marta Sundari[1], Kusman Sadik[2*], Aji Hamim Wigena[2], Anwar Fitrianto[2], Rizaldi Boer[3], Zulkarnain[4]

[1] Study Program on Statistics and Data Science, IPB University, Gd. FMIPA Jl. Meranti Kampus Dramaga Bogor, Indonesia; [2] Study Program on Statistics and Data Science, IPB University, Indonesia 2, Gd. FMIPA Jl. Meranti Kampus Dramaga Bogor, Indonesia; [3] Department of Meteorology and Geophysics, IPB University 5, Gd. FMIPA Jl. Meranti Kampus Dramaga Bogor, Indonesia; [4] Department of Forestry, Faculty of Forestry and Environmental Science, Universitas Halu Oleo. Jl. H.E.A. Mokodompit, Kendari 93121, Southeast Sulawesi, Indonesia.

[*)] Correspondence: kusmans@apps.ipb.ac.id

Citation:

Sundari, M., Sadik, K., Wigena, A. H., Fitrianto, A., Boer, R., Zulkarnain. (2026). Assessing Household Climate Resilience Index to Climate Change Impacts in DKI Jakarta: A Robust Geographically Weighted PCA Approach. Forum Geografi. 40(3), 462-488.

Article history:
Received: 24 March 2026
Revised: 30 June 2026
Accepted: 6 August 2026
Published: 10 August 2026

Abstract

Household climate resilience is spatially heterogeneous because households experience different combinations of exposure, sensitivity, and adaptive capacity across urban settings. This study developeds a local Household Climate Resilience Index (HCRI) for DKI Jakarta using Robust Geographically Weighted Principal Component Analysis based on the Minimum Covariance Determinant estimator (Robust GWPCA-MCD). The analysis used 221 mainland household observations from 17 urban villages in five municipalities of DKI Jakarta, based on the 2022 household resilience survey conducted by CCROM-SEAP IPB University and DLH DKI Jakarta. The final index was constructed using 30 indicators representing exposure, sensitivity, incremental adaptation, and transformational adaptation. Classical GWPCA and Robust GWPCA-MCD were compared to evaluate whether robust local covariance estimation improved the local information structure of the index. The results showed that the Robust GWPCA-MCD produced a substantially stronger local PC1 structure than the classical GWPCA. The classical GWPCA generated a median local PC1 variance of only 14.81%, whereas the Robust GWPCA-MCD increased the median local PC1 variance to 83.66%, with values ranging from 63.42% to 99.999%. The selected model used an adaptive bisquare kernel with 96 nearest neighbors, MCD $\alpha = 0.75$, and an approximate local h-subset of 72 observations. The HCRI classification identified 43 households (19.46%) as extremely low resilience, 12 households (5.43%) as very low, 52 households (23.53%) as low, 58 households (26.24%) as high, and 56 households (25.34%) as very high, with no household classified as extremely high. Spatial mapping showed that the lower and higher resilience categories were unevenly distributed across sampled urban villages. Local loading analysis further revealed that exposure indicators, particularly distance to flood sources, and sensitivity indicators, including housing characteristics, land area, medication expenditure, and post-drought health burden, dominated different local HCRI structures. These findings demonstrate that the Robust GWPCA-MCD provides a statistically robust and spatially interpretable framework for identifying local household resilience profiles and supporting targeted urban climate adaptation planning.

Keywords: Household Climate Resilience Index; Robust GWPCA; Minimum Covariance Determinant; Multivariate outliers; Spatial heterogeneity.

1. Introduction

Climate change is accelerating multi-hazard risks while narrowing the practical window for effective adaptation, making resilience not only a scientific concept but also a pressing planning requirement (IPCC, 2022; Lee *et al.,* 2023; McPhearson *et al.,* 2022; Schipper *et al.,* 2022; Townend *et al.,* 2024). In coastal megacities, climate threats are rarely experienced uniformly. Instead, they are mediated by land-use change, unequal infrastructure provision, and sociospatial inequalities that shape who is exposed, who is protected, and who can recover. This has pushed urban resilience research toward policy-relevant measurement frameworks that are both action oriented and equity aware, positioning justice and distributional effects as core components of resilience rather than peripheral concerns (Sharifi, 2023; Suárez *et al.,* 2024). Evidence syntheses also increasingly emphasize the role of nature-based solutions (NbS) as part of urban adaptation portfolios, particularly for heat and flood risk reduction, but highlight that benefits depend strongly on local implementation capacity and spatial targeting (Ferrario *et al.,* 2024; Mosisa *et al.,* 2025). Collectively, these trends imply that resilience measurement must be simultaneously comparable, spatially targeted, and interpretable for planning decisions that prioritize equity. From a measurement standpoint, this requirement implies a dimensionality reduction challenge: many correlated indicators must be summarized into a smaller set of latent dimensions or a single index, while minimizing information loss and preserving interpretability (Jolliffe & Cadima, 2016). However, for household-scale climate resilience, dimensionality reduction must remain theoretically anchored because a resilience index should not merely summarize statistical variability but should represent a defensible resilience construct. Subiyanto *et al.* (2020) emphasize that climate resilience measurement should be developed from the linked concepts of vulnerability, risk, and resilience, so that indicators reflect exposure, sensitivity, adaptive capacity, and the ability to maintain or transform functions under climate-related stress.

A major methodological response to these demands is the proliferation of index-based resilience and vulnerability frameworks designed to translate complex multidimensional conditions into measurable and comparable metrics. Recent studies have illustrated this shift across diverse systems and scales, including socio-ecological resilience indices for multi-hazard coastal exposure (Mafi-Gholami *et al.,* 2026), livelihood resilience capacity and its determinants (Albore *et al.,* 2025; Subiyanto *et al.,* 2020), composite port resilience indices focused on climate hazards (Polydoropoulou *et al.,* 2025), and multidimensional indices for global climate vulnerability and resilience (Fajardo Gonzalez *et al.,* 2025). Urban applications use index-based approaches to operationalize climate resilience at the city scale (Pécsinger *et al.,* 2025), whereas sectoral work shows how composite indices can capture adaptive capacity and vulnerability in production systems (Singh *et al.,* 2025). Earlier research on urban flood resilience further demonstrated that index-based approaches can be integrated into planning by linking resilience dimensions to actionable interventions (Bertilsson *et al.,* 2019). Collectively, these studies establish that indices can be powerful policy instruments; however, their credibility depends on transparent weighting, robustness to imperfect data, and interpretability in heterogeneous urban settings. Accordingly, a defensible index should clarify (i) how weights are obtained, (ii) how sensitive the results are to data imperfections, and (iii) how dominant components map onto substantive resilience meaning. In practice, these requirements imply that an index method should provide (a) an explicit statistical mechanism for deriving weights, (b) diagnostics for how well a low-dimensional summary represents the original indicator space, and (c) stable output under plausible data contamination (Jolliffe & Cadima, 2016). In addition, because resilience is multidimensional and context dependent, index construction should explicitly explain the direction of each indicator, especially when vulnerability-oriented indicators, such as exposure and sensitivity, are transformed into resilience-oriented constructs, such as non-exposure and low sensitivity (IPCC, 2022; Subiyanto *et al.,* 2020).

Jakarta is a salient case where these requirements become particularly acute. As a rapidly urbanizing coastal megacity, Jakarta faces intersecting climate and developmental pressures, including recurrent flood risks and long-documented land subsidence processes that intensify coastal and pluvial flood impacts and complicate adaptation planning (Abidin *et al.,* 2011). Recent evidence has confirmed that land subsidence remains spatially uneven across Greater Jakarta, with stronger subsidence patterns observed in the coastal and northern parts of Jakarta, thereby reinforcing the need for spatially explicit resilience assessments (Bott *et al.,* 2021; Harintaka *et al.,* 2024). Household resilience in Jakarta is, therefore, inherently spatial: exposure and service accessibility vary across neighborhoods, and adaptive capacity can be strongly conditioned by local institutional support, infrastructure quality, and socioeconomic constraints. This implies that a single global resilience structure may obscure important local patterns, precisely the patterns most relevant for neighborhood-scale targeting and equitable policy design. For planning, this spatial heterogeneity is not a methodological nuance but a core requirement: interventions must be allocated to where deficits concentrate and to which indicator groups dominate locally. Consequently, resilience measurement in Jakarta requires methods that can estimate locally varying structures, rather than assuming spatial stationarity in indicator relationships (Harris *et al.,* 2011). This is particularly relevant for DKI Jakarta because household resilience may vary not only between municipalities but also between urban villages within the same municipality, depending on local combinations of hazard exposure, housing conditions, water access, household economic capacity, health vulnerability, and adaptation practices.

A key technical challenge in resilience index construction is indicator weighting because weighting determines how observed variables translate into composite scores and household rankings. Expert-driven weighting can incorporate contextual knowledge but may suffer from subjectivity and limited reproducibility across studies and settings. In contrast, Principal Component Analysis (PCA) offers a widely used data-driven alternative that derives weights from the covariance structure, enabling replicable dimensionality reduction and composite scoring (Jolliffe & Cadima, 2016). However, classical PCA is sensitive to outliers and leverage points because it relies on the empirical covariance matrix; even modest contamination can tilt principal directions and distort explained variance, which may in turn bias derived weights and household classifications. In index construction, the proportion of variance explained by the first principal component (PC1) can serve as a practical indicator of how well a one-dimensional score represents the dominant multivariate structure. Nevertheless, explained variance should not be treated as the sole criterion of methodological adequacy. To ensure credibility, percentage PC1 (%PC1) evidence must be accompanied by a substantive interpretation of PC1 through dominant loadings and stability checks of household rankings under plausible perturbations, such as outlier resistance and alternative spatial settings. Because PC1 is a one-dimensional projection that maximizes variance, a high %PC1 provides a direct, data-driven indication that the index captures a large share of the dominant information in the original multivariate indicator space, thereby reducing information loss in one-score scaling (Jolliffe & Cadima, 2016). However, a high %PC1 does not automatically imply that PC1 is substantively valid as a resilience index. The direction of PC1, the signs of local loadings, and the dominant indicators must be aligned with the theoretical meaning of resilience so that higher HCRI scores consistently represent higher household resilience rather than merely larger numerical variation.

Robust multivariate statistics address this issue by replacing classical covariance with resistant scatter estimators. The Minimum Covariance Determinant (MCD) estimator is one of the most established approaches, supported by computationally efficient algorithms that make robust covariance estimation feasible in applied research (Rousseeuw & Driessen, 1999). Methodological reviews further clarify how MCD and its extensions provide high breakdown estimation under contamination and serve as a principled basis for robust PCA in practice (Hubert *et al.,* 2018). For household survey-based resilience measurement, this is critical: robust scatter estimation helps ensure that composite indices reflect a dominant multivariate structure rather than being driven by a small set of extreme households. In other words, robustness supports trustworthy weighting by reducing the risk that a few atypical households disproportionately define the index direction and score ordering. More broadly, MCD-based estimation is widely used as a robust foundation for both outlier detection and robust multivariate structure learning, particularly following the development of computationally efficient FastMCD-type algorithms (Hubert *et al.,* 2018). In household resilience data, observations flagged by a robust Mahalanobis distance should be interpreted carefully because extreme multivariate profiles may represent true household heterogeneity, unequal hazard experience, or socioeconomic diversity, rather than simple measurement errors.

A previous study by Sundari *et al.* (2026) developed the Household Climate Resilience Index (HCRI) for DKI Jakarta using a global Robust PCA MCD framework. This study used 221 mainland households from 17 urban villages and operationalized household climate resilience through four dimensions: exposure, sensitivity, incremental adaptation, and transformational adaptation. The sampling design and selected urban villages were based on an urgency-based vulnerability stratification derived from Jakarta's multi-hazard climate risk profile, including flood, drought, tidal inundation, and extreme heat. Sundari *et al.* (2026) provided the first robust global HCRI framework for mainland Jakarta, whereas the present study extends this framework by adding a geographically weighted structure to the PCA process. This positioning is important because the present study does not rebuild the HCRI concept from the beginning; instead, it develops a second-stage analysis by examining whether the HCRI structure varies spatially and identifying the indicators that dominate the local resilience structure in each location.

However, robustness alone is insufficient when resilience is spatially nonstationary. Geographically weighted PCA (GWPCA) extends PCA by estimating local covariance structures via spatial kernels and bandwidths, allowing principal components and loadings to vary across space and enabling the mapping of geographically distinct multivariate patterns (Harris *et al.,* 2011; Lu *et al.,* 2025). This is consistent with the needs of applied geography: identifying where resilience deficits are concentrated and which indicator groups dominate in different localities. Practical implementation is also supported by established software ecosystems for geographically weighted analysis (Gollini *et al.,* 2015). However, classical GWPCA can still be undermined by localized outliers within moving windows and by small effective local sample sizes, which can destabilize local loadings and spatial interpretations. This creates practical tension in household-level applications: the localization needed to reveal neighborhood patterns can amplify sensitivity to local anomalies unless robust local scatter estimation is used. Empirical and methodological studies also note that GWPCA outputs can vary discontinuously across space in certain settings, reinforcing the need for careful bandwidth calibration and robust local covariance estimation when interpreting mapped component structures (Tsutsumida *et al.,* 2022). Therefore, integrating GWPCA with MCD-based robust covariance estimation is useful for constructing a spatially adaptive HCRI that is both sensitive to local heterogeneity and resistant to multivariate extreme profiles.

Despite the rapid growth in resilience indices and the maturity of geographically weighted multivariate methods, household-level resilience assessment in megacities rarely integrates (i) data-driven weighting, (ii) explicit spatial non-stationarity, and (iii) outlier resistance in a single, transparent, and reproducible workflow. Therefore, many studies either apply robust PCA without spatial localization, masking heterogeneity; apply GWPCA without robust local scatter estimation, exposing results to local anomalies; or interpret indices mainly through explained variance without sufficiently linking dominant components to substantive resilience meanings. This study addresses this limitation by treating %PC1 as a necessary, but not sufficient, diagnostic for index suitability and by explicitly connecting local PC1 structures to interpretable indicator groups and to the stability of household classifications across space. This integrated framing also responds to the practical demand in planning contexts: indices must not only summarize variation but also do so in a way that is stable, mappable, and explainable to decision-makers at the neighborhood scale (Lu *et al.,* 2025). In this study, the local loading structure is central because it allows identifying location-specific dominant indicators. This means that the HCRI is interpreted not only as a resilience score but also as a diagnostic tool for understanding whether resilience in each urban village is shaped more strongly by exposure, sensitivity, incremental adaptation, or transformational adaptation indicators.

Therefore, this study aimed to construct a HCRI for DKI Jakarta using a Robust GWPCA framework that combines geographically weighted local PCA with MCD-based local covariance estimation (Harris *et al.,* 2014), producing household scores that are simultaneously spatially sensitive and resistant to contamination. The contribution is threefold: (1) a reproducible robust–spatial index construction workflow suitable for household survey data; (2) locally varying resilience patterns that support municipality- and neighborhood-level targeting; and (3) an interpretable diagnostic of dominant indicators via local loadings to better connect statistical outputs to actionable policy levers in Jakarta's socio-spatial context. Compared to the previous global HCRI study, an additional contribution of the present study is its ability to reveal dominant resilience indicators per location; therefore, place-based interventions can be linked to the local structure of household resilience rather than to a single global pattern. In this framing, "best performance" is not defined only by maximizing %PC1, but by jointly achieving high information capture, interpretable dominant indicators, and stable household rankings under contamination and spatial non-stationarity. To make the methodological contribution auditable and reproducible, this study reports key model settings, including the kernel/bandwidth strategy and robust covariance choices, and uses %PC1 together with loading-based interpretation as complementary evidence for index suitability rather than a single decisive criterion (Jolliffe & Cadima, 2016). Thus, Robust GWPCA MCD is positioned as a spatial extension of Robust PCA MCD, not as a method that is superior merely because it produces higher local PC1 variance.

The remainder of this paper is organized as follows. Section 2 describes the study area, data, preprocessing, and model settings. Section 3 presents the results, including data characteristics, robust Mahalanobis distance, local PC1 variance, HCRI classification, and location-specific dominant indicators. Section 4 discusses the methodological and substantive implications of the findings, including robustness, policy interpretation, and limitations. Section 5 concludes with the main contributions, empirical findings, limitations, and future research directions. This structure is intended to keep the link between statistical design choices and planning interpretation explicit; model settings and diagnostics are presented before spatial maps and classification outputs to support a transparent reading of the index results (Harris *et al.,* 2011).

2. Research Methods

2.1. Study Area

Jakarta is located on the island of Java, which lies along the Pacific Ring of Fire, rendering it susceptible to natural hazards, such as flooding, land subsidence, and earthquakes. As a highly dense metropolis, Jakarta is also prone to non-natural hazards, particularly urban fires. The Indonesian Disaster Risk Index (IRBI) for DKI Jakarta in 2021 was 60.43, placing the province in the medium-risk category (BPBD, 2021). A downward trend in the IRBI has been observed since 2015, reflecting the efforts of the Provincial Government of DKI Jakarta to strengthen regional resilience and stability against disaster risks. The safety of residents and the security of Jakarta remain top priorities, as evidenced by a range of mitigation policies, infrastructure strengthening, and enhanced community preparedness to face potential disasters.

Jakarta is located between 5°19′12″ - 6°23′54″ S and 106°22′42″ and 106°22′42″-106°58′18″ E, with an average elevation of approximately 7 meters above sea level and a total area of 662.33 km². Jakarta is the capital of the Republic of Indonesia and comprises five administrative municipalities and one administrative regency, with a total area of 662.33 km². Administratively, the province comprises five municipalities and one administrative regency, subdivided into 44 districts and 267 urban villages (Bappeda Jakarta, 2018). The southern and eastern boundaries adjoin Depok City, Bogor Regency, Bekasi City, and Bekasi Regency; the western boundary adjoins Tangerang City and Tangerang Regency; and the northern boundary is Java Sea.

This geographic setting is important for the present study because climate-related hazards in Jakarta are spatially heterogeneous. Northern and coastal areas are more strongly affected by tidal inundation, recurrent flooding, and land subsidence, whereas inland areas may experience different combinations of flood, drought, heat, infrastructure constraints, and socioeconomic exposure. Therefore, Jakarta provides an appropriate case for applying a geographically weighted multivariate approach, because household resilience is expected to vary across local spatial contexts rather than following a single global structure.

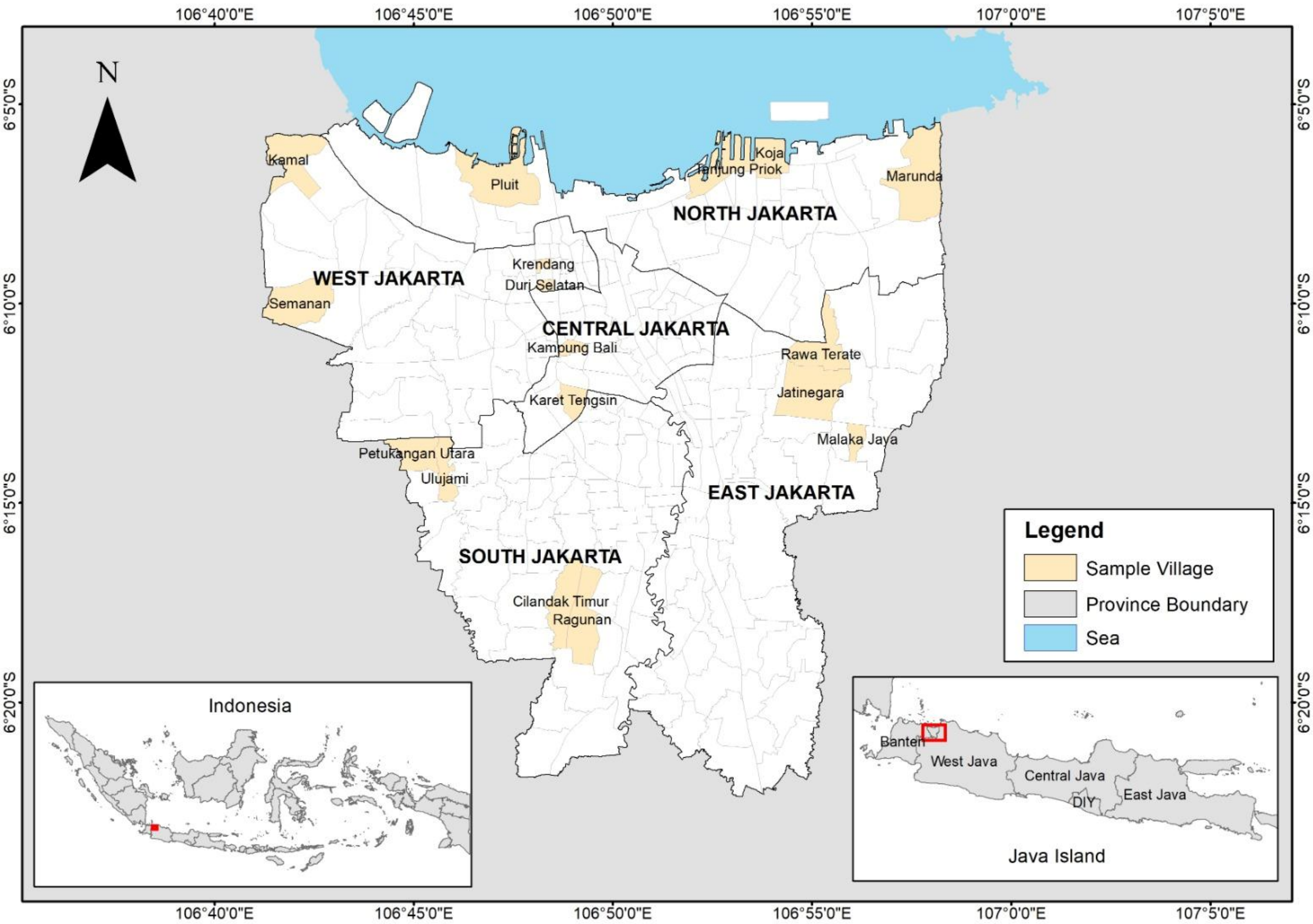

Figure 1. Map of Study Area.

2.2. Data Source, Survey Design, and Unit of Analysis

This study used household survey data collected in 2022 by CCROM-SEAP (IPB University) in collaboration with the Jakarta Environmental Agency (Boer *et al.,* 2022). Survey locations were determined by an urgency assessment derived from the risks of flood, drought, tidal inundation, and extreme temperature (Dinas Lingkungan Hidup Provinsi DKI Jakarta, 2021). The distribution of urban villages across vulnerability levels under each urgency scenario is summarized in Table 1. Based on this urgency framework, 17 mainland urban villages were selected to represent urgency levels and municipalities in Jakarta; the distribution of these selected villages across vulnerability levels is presented in Table 2.

Jakarta's population reached 10,609,781 in 2021, with an annual growth rate of 0.57%. It is the most densely populated province in Indonesia, with a population density of 15,978 persons per km² (BPS Jakarta, 2022). This survey used stratified random sampling, and the survey sample size was determined using Slovin's formula based on a population of 2,770,729 households and a margin of error of 5%, resulting in 400 respondents (Boer *et al.,* 2022). The 400 respondents comprised 221 mainland households, 26 island households, and 143 business units drawn from 17 mainland and 4 island villages.

This study is a methodological extension of the previously published HCRI study by Sundari *et al.* (2026), who developed a household resilience index using a global Robust PCA-MCD framework. The present study uses the same mainland household dataset but extends the analysis by incorporating a geographically weighted structure into the PCA. Therefore, the sampling design, selected urban villages, and unit of analysis followed those of Sundari *et al.* (2026). In the previous study, the selected urban villages were not determined merely by administrative representation but were based on an urgency-based vulnerability stratification derived from Jakarta's multi-hazard climate risk profile, including flood, drought, tidal inundation, and extreme heat.

This study focuses on the 221 mainland households to ensure adequate local support (i.e., a sufficient number of neighbors) for geographically weighted principal component analysis (GWPCA). The respondents were selected to represent three income groups—lower-middle, middle, and upper-middle—to capture income-based heterogeneity in climate change impacts. The income groups were justified by the enumerators based on the household's residential location (informal/slum areas, non-exclusive housing estates, and exclusive gated clusters) and the physical characteristics of the dwelling structure (permanent vs. non-permanent).

Table 1. Distribution of Urban Villages Across Vulnerability Levels by Urgency Scenario.

No.	Urgency	Type of Urgency				Population Vulnerability Level 1	2	3	4	5	6	7	Number of Urban Villages
1	1a	Flood	Drought	Tidal Flood							1		1
2	1b	Flood	Drought		Extreme heat			1	5	2			8
3	1c	Flood		Tidal Flood	Extreme heat							3	3
4	2a	Flood	Drought						2		1		3
5	2b	Flood		Tidal Flood					1	3	1		5
6	2c	Flood			Extreme heat			2	8	5	3	1	19
7	2d		Drought	Tidal Flood							1		1
8	2e		Drought		Extreme heat			5	1	1			7
9	3a	Flood						2	9	6	6	2	25
10	3b		Drought						1	1			2
11	3c			Tidal Flood				1		4	5	2	12
12	3d				Extreme heat			13	20	5	1		39
13	4-					8	31	54	31	9	3		136

Table 2. Distribution of Selected Urban Villages Across Vulnerability Levels.

No.	Urgency	Sample Number of Urban Villages	Vulnerability Level 1	2	3	4	5	6	7
1	1a	1						Koja	
2	1b	1					Cilandak Timur		
3	1c	1							Kamal
4	2a	1						Rawa Terate	
5	2b	1						Tanjung Priok	
6	2c	2					Petukangan Utara		Semanan
7	2d	1						Marunda	
8	2e	1				Duri Selatan			
9	3a	2			Karet Tengsin				Jatinegara
10	3b	1					Kampung Bali		
11	3c	1			Pluit				
12	3d	2			Ulujami	Krendang			
13	4-	2	Ragunan	Malaka Jaya					

Legends:

West Jakarta | North Jakarta | South Jakarta | Central Jakarta | East Jakarta

The restriction to 221 mainland households is analytically important for two reasons. First, business units were excluded because their exposure pathways, decision-making logic, and adaptation strategies differed from those of households. Second, island households were excluded because their geographic exposure, governance settings, and infrastructure conditions differed from those in mainland Jakarta. Thus, the analytical unit used in this study was the mainland household.

However, because the sample represents 221 households from 17 of 267 urban villages in Jakarta, the findings should be interpreted as evidence for the selected mainland urban villages rather than as a full generalization to all households or all urban villages in DKI Jakarta. This representativeness constraint is acknowledged as a structural limitation and is discussed further in the Discussion section.

2.3. Resilience Framework and Indicators Set

Household climate resilience is operationalized using four dimensions–exposure, sensitivity, incremental adaptive capacity, and transformational adaptive capacity–implemented through 45 household-level indicators derived from the survey instrument and organized across thematic sectors relevant to climate risk and adaptive capacity (Boer *et al.,* 2022). Following the resilience framework in the literature (Subiyanto *et al.,* 2020), these dimensions are expressed as (i) non-exposure (geographic–demographic conditions related to flood/drought hazards), (ii) low sensitivity (dwelling conditions, health, and water resources), (iii) incremental adaptation (economic conditions and human resources), and (iv) transformational adaptation (personal/household practices). The complete indicator list, sector mapping, coding, and measurement types are presented in Table 3.

In conventional vulnerability analysis, higher exposure and higher sensitivity indicate greater vulnerability. In the present resilience-oriented framework, the directions of these indicators are aligned such that higher transformed values consistently represent more resilient conditions. Thus, exposure indicates lower household exposure to climate-related hazards after indicator orientation, whereas low sensitivity indicates lower internal susceptibility of households, housing conditions, health conditions, and water-resource conditions to climate impacts.

Incremental adaptation refers to household coping and adjustment capacity under current climate stress, such as economic resources, human resources, and actions that reduce immediate losses. Transformational adaptation refers to broader household practices and behavioral changes that may strengthen the long-term adaptive capacity under future climate uncertainty. This distinction is important because the HCRI is not intended to measure exposure alone, material assets alone, or vulnerability alone, but rather the combined household capacity to avoid, withstand, cope with, and adapt to climate-related disturbances.

As shown in Table 3, the final indicator set used to construct the HCRI consists of 30 indicators, comprising 17 numeric variables and 13 categorical variables. The numeric indicators were directly included in the PCA/GWPCA input matrix, whereas the 13 categorical indicators marked as MSI = "Yes" in Table 3 were transformed into interval-scale scores using the Method of Successive Intervals (MSI) prior to covariance-based PCA/GWPCA. Only categorical variables with a meaningful ordinal structure, or variables that had been theoretically recoded into ordered resilience levels, were treated using MSI. Nominal variables were not directly interpreted as ordinal unless their categories had a defensible resilience ordering. This clarification was added to avoid inappropriate treatment of unordered categorical variables in the PCA input matrix.

2.4. Data Pre-Processing

Before the analysis, the study conducted data pre-processing in three steps. First, because PCA requires numerical inputs, while the questionnaire includes categorical responses (Boer *et al.,* 2022), the 13 ordinal indicators in Table 3 were transformed into interval-scale scores using the MSI (Green, 2017). This transformation produces continuous scores that preserve the original response ordering, allowing ordinal and numeric indicators to be analyzed jointly in the subsequent PCA computation. The MSI was applied only to categorical variables with a meaningful ordinal structure or to variables that had been theoretically recoded into ordered resilience levels. Nominal variables were not treated directly as ordinal unless their categories had a defensible resilience ordering.

Established PCA variants for categorical-only and mixed-type data are available, particularly for categorical PCA/nonlinear PCA via optimal scaling and mixed-data approaches, such as PCAmix or FAMD (Chavent *et al.,* 2022; Pagès, 2014). A preliminary sensitivity analysis using PCAmix showed that the first dimension explained only 6.26% of the total variation, with a cumulative proportion of 6.26%. This result indicates that the first PCAmix dimension did not provide a sufficiently dominant one-dimensional structure for constructing a single HCRI. Therefore, MSI-based intervalization was retained because it produced a coherent numerical input matrix for covariance-based PCA and GWPCA, while preserving the theoretical ordering of ordinal resilience indicators. This choice is consistent with the objective of this study, namely to construct an interpretable one-number HCRI based on the dominant local principal component.

Table 3. Indicators Used in Constructing the Household Climate Resilience Index.

Indicator	Sector	No.	Code	Variable	Data Type	MSI
Exposure	Geographical conditions	1	C2b	Distance of the house to the main flood source	Numeric	No
		2	C3b	Distance to other flood sources	Numeric	No
		3	C4	Amount of day flood in the past years	Numeric	No
		4	F1	House elevation to street	Numeric	No
Sensitivity	Health	5	E11	Proportion of sick family members after flood	Numeric	No
		6	E14	Medication expenditure	Numeric	No
		7	I5	Proportion of sick family members after drought	Numeric	No
		8	N2	Proportion of sick family members with dengue	Numeric	No
	Residence	9	B3	Building area	Numeric	No
		10	B4	Land area	Numeric	No
		11	B5	House building structure	Categorical	Yes
		12	B6	Floor type	Categorical	Yes
		13	B7	Roof type	Categorical	Yes
		14	F2	Permanent dike height at main entrance	Numeric	No
		15	F7	Flood water height for evacuation	Numeric	No
	Water sources	16	E9	Cost of buying water after a flood	Numeric	No
		17	G1	Water source for toilet	Categorical	Yes
		18	G6	Water source for drinking	Categorical	Yes
		19	I3	Post-drought water expenditure	Numeric	No
Incremental Adaptation	Economics	20	A14	Expenses per family member	Numeric	No
		21	A6	Main Occupation: Head of the family	Categorical	Yes
		22	B2	Number of floors	Categorical	Yes
		23	D3	Household actions to reduce flood loss	Categorical	Yes
	Human Resources	24	A4	Final education	Categorical	Yes
		25	A5	Proportion of working-age household members	Numeric	No
		26	O2	Frequency of routine examination of jumantic officers	Categorical	Yes
		27	O3	Frequency of puddle cleaning	Categorical	Yes
Transformational Adaptation	Personal	28	D2	Flood loss mitigation efforts	Categorical	Yes
		29	E4.1	Number of people cleaning the house	Numeric	No
		30	J2	Drought adaptation efforts	Categorical	Yes

Second, the study retained the final HCRI indicators on their original oriented scales after the required MSI transformation. No additional manual global centering, local centering, or standardization transformation was applied to the full input matrix before the main GWPCA and Robust GWPCA-MCD estimation. This decision was made because the study aimed to preserve the empirical variation in the original household data and facilitate interpretation of the resulting PC scores in relation to household-level differences. Several indicators, such as distance to flood sources, number of flood days, house elevation, building area, land area, health-related proportions, and household expenditures, contain substantively meaningful magnitude information. Standardizing or centering the full input matrix prior to model estimation could reduce the direct interpretability of these original-scale household differences.

This choice means that the main analysis follows a covariance-based GWPCA specification and is scale-dependent. Indicators with larger empirical variance may contribute more strongly to the extracted components. Therefore, the results cannot be interpreted as being free from scale effects. Instead, the covariance-based results are interpreted together with indicator-scale diagnostics, loading interpretation, local support diagnostics, and robustness checks. The dominant indicators are interpreted as statistical contributors to the local covariance structure rather than as causal determinants of household resilience.

Third, multivariate outliers were screened using the robust Mahalanobis distance to reduce the influence of extreme observations on covariance estimation and the resulting principal component directions. In the classical formulation, the Mahalanobis distance is computed from the sample mean vector and covariance matrix and can be compared against a reference cutoff, such as a chi-square quantile with degrees of freedom equal to the number of variables (Filzmoser & Gregorich, 2020; Johnson & Wichern, 2019; Maronna *et al.,* 2019). However, because classical estimates are sensitive to contamination and may lead to masking and swamping when multiple outliers are present, this study employed the MCD estimator to obtain robust estimates of location and scatter and compute robust Mahalanobis distances for outlier flagging.

The robust Mahalanobis distance was calculated using a 13-variable numerical subset selected for outlier detection. This subset was not identical to the full GWPCA indicator set. The full GWPCA model used 30 final indicators after transformation and screening, whereas $p = 13$ was used only as the degrees of freedom for the robust Mahalanobis distance cutoff. This distinction was added to avoid confusion between the outlier-detection and the final HCRI construction stages.

Observations flagged by robust Mahalanobis distance were not automatically excluded from the analysis. Because 41.6% of households were flagged, the results were interpreted as evidence of strong multivariate heterogeneity rather than simple data contamination. These flagged households may reflect true diversity in household exposure, housing conditions, health burden, economic resources, and adaptation practices. Therefore, robust methods were used to reduce their leverage in the covariance estimation while preserving them as part of the empirical household resilience structure.

Fourth, potential multicollinearity or redundancy among the indicators was assessed using the Variance Inflation Factor (VIF) (Upendra *et al.,* 2023). The VIF quantifies the extent to which a variable can be linearly explained by the remaining variables; values close to 1 indicate negligible collinearity, whereas larger values indicate increasing redundancy and inflated standard errors. Indicators with high VIF values were treated as candidates for further handling, such as removal or consolidation, prior to PCA to improve numerical stability and support a clearer interpretation of the extracted components.

In this study, the VIF was used only as a preliminary redundancy diagnostic, not as a replacement for PCA diagnostics. As VIF is more commonly associated with regression diagnostics, its role in this study was limited to identifying near-linear redundancy among the candidate indicators before robust covariance estimation. The final indicator decision was based on a combination of the VIF results, theoretical relevance, measurement type, data completeness, and interpretability within the HCRI framework.

2.5. Robust GWPCA

GWPCA extends global PCA by allowing the multivariate structure of the data to vary across space, thereby capturing spatial heterogeneity in the dominant patterns of covariation. For a data matrix $\boldsymbol{X}$ and a target location $(u_{i'} v_i)$, observations are weighted according to their geographic proximity via a kernel function, PCA is performed on the resulting locally weighted variance–covariance structure, and the degree of localization is governed by the bandwidth parameter (Harris *et al.,* 2011; Lu *et al.,* 2025). The geographically weighted variance–covariance matrix at $(u_{i'} v_i)$is defined as Equation 1:

$$\Sigma(u_i, v_i) = X^\top W(u_i, v_i)X, \tag{1}$$

where $W(u_i, v_i)$ is a diagonal matrix of spatial weights. Local principal components are then obtained by eigendecomposition of $\Sigma(u_i, v_i)$, yielding location-specific eigenvalues, loadings, and component scores that can be mapped to interpret geographic variation in the dominant dimensions of the dataset (Harris *et al.,* 2011; Lu *et al.,* 2025).

To reduce sensitivity to multivariate outliers and spatially varying leverage points, this study applies robust GWPCA, replacing the classical locally weighted covariance with a robust estimator. This robust specification is intended to produce more stable local eigenstructures under contamination, thereby strengthening the inference about spatial patterns derived from localized components (Harris *et al.,* 2012). Specifically, both the local mean vector $\mu(u_i, v_i)$ and the local covariance matrix $\Sigma(u_i, v_i)$ are estimated using the MCD estimator at each location (Hubert *et al.,* 2018). The MCD seeks a subset of observations with minimal covariance determinants and subsequently applies a standard reweighting step to improve statistical efficiency, reducing the influence of atypical observations on the local covariance matrix used for PCA. In implementation, the MCD solution is computed using the FAST-MCD procedure in standard software, with robustness controlled through the subset size h(or equivalently α) and a chi-square cutoff for robust distances (Hubert *et al.,* 2018; Rousseeuw & Driessen, 1999).

The MCD tuning parameters, including the selected alpha value, corresponding h-subset size, reweighting procedure, and robust-distance cutoff, were reported to improve reproducibility. Because robust local covariance estimation depends on the relationship between the local sample size and the number of variables, local support was also evaluated using the number of neighboring observations and the effective local sample size at each target location.

Spatial data were managed as spatial objects in R, and inter-location distances were derived from household coordinates to construct $W(u_i, v_i)$ through an explicit distance matrix. Because locations are recorded in longitude–latitude, distances were computed using spherical (great-circle) distance so that geographic separation is measured on the Earth's surface rather than on a planar projection. A bi-square kernel was then applied to assign higher weights to nearer observations and smoothly downweight more distant observations, thereby emphasizing localized covariance structures while preserving spatial continuity on the weighting surface (Harris *et al.,* 2011; Lu *et al.,* 2025).

The bandwidth in GWPCA may be specified either as a fixed distance or as an adaptive number of nearest neighbors (Harris *et al.,* 2011; Lu *et al.,* 2025). This study adopts a fixed bandwidth because preliminary comparisons indicated that the adaptive specification produced a lower proportion of variance explained by the first component (PC1), which is the primary quantity required for index construction. Bandwidth selection was guided by cross-validation (CV). To align computation with the index-construction objective, only the first two components were retained during bandwidth tuning and estimation, whereas substantive interpretation focused on PC1.

Bandwidth selection was not justified solely by maximizing the percentage of variance explained by PC1 because doing so would create circular reasoning when PC1 is also used as the index basis. Therefore, the revised bandwidth justification combines several criteria: cross-validation, local loading stability, a sufficient effective local sample size, and classification stability across reasonable bandwidth alternatives. The selected bandwidth was reported together with the cross-validation results and the sensitivity of local PC1 variance and dominant loadings.

Robust GWPCA was implemented by replacing the classical locally weighted covariance with an MCD estimator to reduce sensitivity to multivariate outliers and spatially varying leverage points (Hubert *et al.,* 2018; Lu *et al.,* 2014; Rousseeuw & Driessen, 1999). All analyses were performed in R. For reproducibility, the revised manuscript should report the exact R version and package versions used for the analysis, including the GW model for geographically weighted modelling, sp for spatial data handling, and the relevant robust multivariate packages used for MCD estimation.

2.6. Index Scaling and Classification

The central methodological issue in constructing an HCRI is dimensionality reduction: a large set of indicators must be summarized into a single, interpretable measure while retaining the most salient information. From a dimensionality-reduction perspective, prioritizing PC1 with the largest explained variance (e.g., exceeding a threshold such as 70%) for HCRI construction is defensible because PC1 is a one-dimensional projection that captures the maximum variance, making its scores the most informative single-number summary when an index must be expressed as one value per household (Jolliffe & Cadima, 2016). In applied index construction using PCA (e.g., wealth/SES indices), early components, often PC1, are used as index scores when they explain a substantial share of the total variance, indicating that the lower-dimensional representation remains strongly aligned with the dominant information in the original indicators (Howe *et al.,* 2008; Vyas & Kumaranayake, 2006).

The overall workflow, from indicator preparation and robust outlier screening to robust GWPCA estimation and PC1-based index scaling and classification, is summarized in Figure 2.

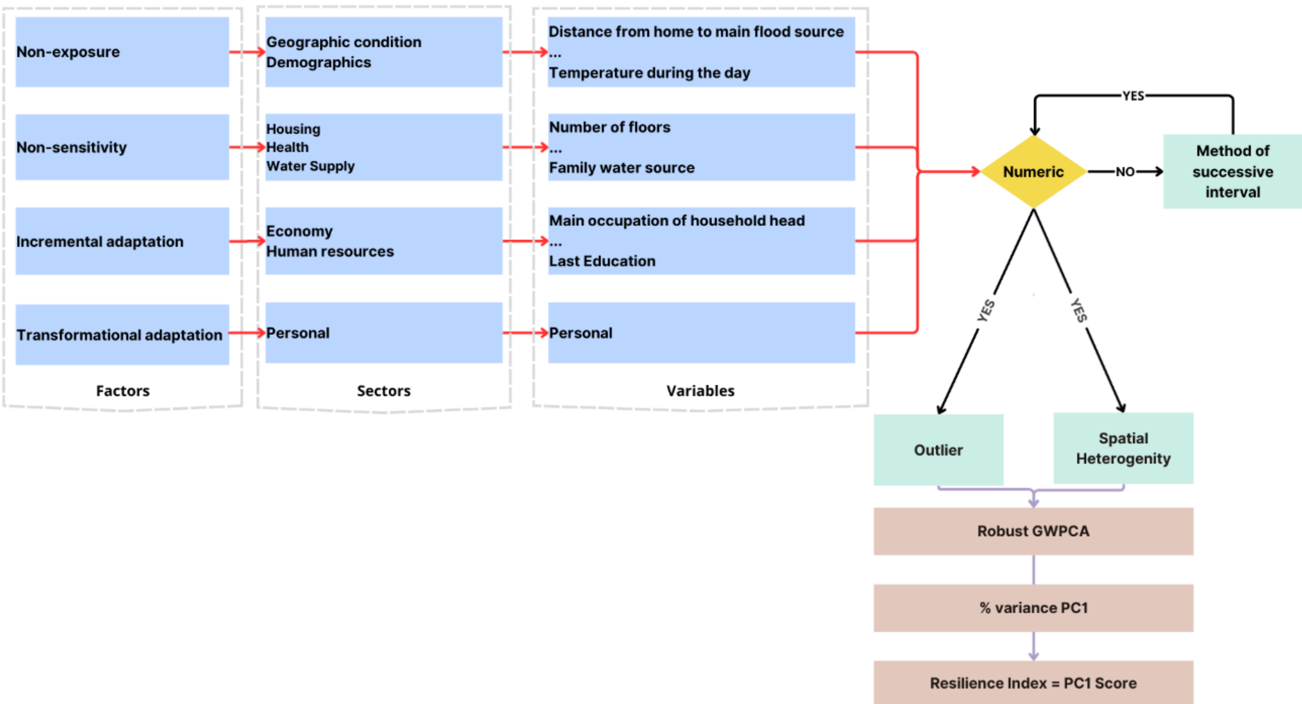

Figure 2. Research Methodology.

Thus, the larger the proportion of variance explained by PC1, the smaller the information loss induced by dimensionality reduction, strengthening the interpretability and defensibility of PC1-based scaling and classification of the HCRI (Howe *et al.,* 2008; Jolliffe & Cadima, 2016). Accordingly, this study reports the GWPCA outputs by resilience dimension, focusing on the proportion of variance explained by PC1 and the associated component structure, as summarized in Table 4.

Table 4. GWPCA Results for Each Resilience Dimension.

Value Range	HCRI
PC1 Score < Lower bound	Very extremely low
Lower bound ≤ PC1 Score < Q1	Very low
Q1 ≤ PC1 Score < Q2	Low
Q2 ≤ PC1 Score < Q3	High
Q3 ≤ PC1 Score < Upper bound	Very high
Upper bound ≤ PC1 Score	Very extremely high

3. Results

3.1. Data Characteristics and Indicator Scale Diagnostics

The final dataset used in this study consisted of 221 mainland household observations and 30 HCRI indicators. These indicators represent the four dimensions of household climate resilience: exposure, sensitivity, incremental adaptation, and transformational adaptation. These dimensions are consistent with the broader climate-resilience framework, which views resilience as the capacity of social units to absorb disturbances, maintain function, and adapt to climate-related stresses (Adger, 2000; IPCC, 2014). Before applying the geographically weighted model, the distribution and scale of the indicators were examined to describe the empirical structure of the data and identify potential issues related to unequal variance, extreme values, and differences in measurement units.

The HCRI indicators were measured on heterogeneous empirical scales. Some indicators represented distances to flood sources, number of flood days, house elevation, household expenditure, land area, building area, health-related proportions, and transformed categorical scores. This structure indicates that the final HCRI dataset combines physical exposure, housing characteristics, health burden, economic capacity, and household adaptation responses. Therefore, the indicators are not homogeneous in terms of unit, range, or variability. This issue is important because PCA is directly influenced by the variance–covariance structure of the input variables, particularly when the analysis is performed using covariance-based estimation (Jolliffe, 2002; Jolliffe & Cadima, 2016).

Several indicators exhibited extreme empirical values. These values were not automatically treated as data errors. Instead, they were interpreted as possible indicators of household heterogeneity across the sampled urban villages. In the context of household climate resilience, unusual values may reflect real differences in flood exposure, distance from hazard sources, housing elevation, land ownership, building size, post-disaster expenditure, and household capacity to respond to climate-related disturbances. This interpretation is important because household-level resilience data may contain atypical but substantively meaningful profiles, rather than simple statistical contamination.

The diagnostic assessment of the indicator distribution is also relevant for GWPCA because the method estimates local principal components from geographically weighted covariance structures. Unlike global PCA, which summarizes the overall covariance structure of the full dataset, GWPCA allows the dominant multivariate structure to vary across locations (Fotheringham *et al.,* 2002; Harris *et al.,* 2011). Consequently, extreme or high-leverage observations located within a local neighborhood may affect local eigenvalues, eigenvectors, component loadings, and PC1 scores more strongly than in a global model.

Therefore, the observed variation in the indicator scale and distribution provides an empirical basis for applying a robust covariance approach in the local PCA framework. Robust GWPCA-MCD was used to reduce the influence of high-leverage observations while retaining household profiles that may be substantively meaningful for resilience assessment. The MCD estimator is commonly used to obtain robust estimates of multivariate locations and scatter in the presence of atypical observations (Rousseeuw, 1984; Rousseeuw & Driessen, 1999). Thus, using a robust local covariance estimator is appropriate for household resilience data that may contain heterogeneous and spatially uneven multivariate profiles. The distribution of the 30 final HCRI indicators is shown in Figure 3. This figure provides a visual diagnostic of the differences in spread, range, and potential extreme values across the indicators. The visual pattern is used as an initial indication that the household resilience data contain heterogeneous multivariate structures, which motivates subsequent comparison between the global PCA baselines and the local Robust GWPCA-MCD framework.

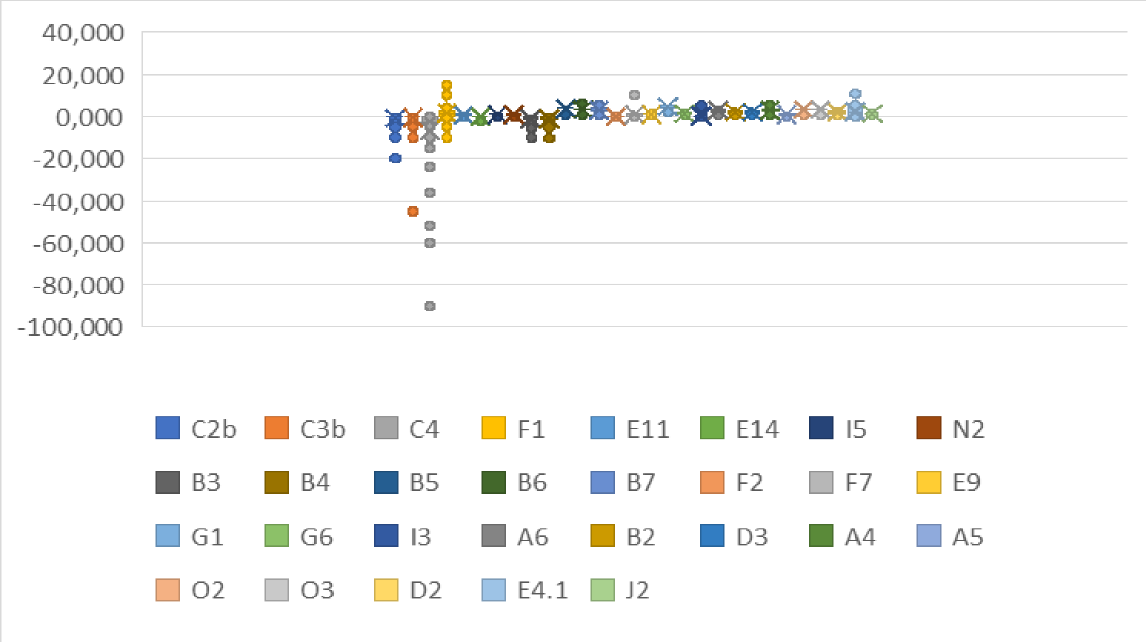

Figure 3. Indicator Value Distribution.

3.2. Global PCA Baseline and Covariance-Based Diagnostic

Before applying the local Robust GWPCA-MCD model, the global PCA was first examined as a baseline diagnostic. This step was used to evaluate whether the final HCRI indicators formed a dominant multivariate structure at the household level. The global PCA result was not intended to replace the spatially local model but to provide a reference point before the covariance structure was allowed to vary geographically. In the subsequent local model, the final analytical setting consisted of 221 household observations, 30 HCRI indicators, two retained components, and a bi-square geographically weighted kernel.

The global PCA baseline showed that two classical PCA formulations, namely, PCA based on singular value decomposition (PCA-SVD) and PCA based on the covariance matrix, produced the same PC1 variance share of 87.46%. This result indicates that the dominant global component was consistent across the two equivalent PCA computations under the same input structure. In the PCA theory, the SVD formulation and eigendecomposition of the covariance matrix are mathematically connected because both identify the orthogonal directions that maximize the variance of the projected data. This relationship is also described by Sundari *et al.* (2026), where PCA is formulated through the eigenvalue problem of the covariance matrix and, equivalently, through the SVD of the column-centered data matrix.

The high PC1 variance from the PCA-SVD and PCA covariance provides an initial indication that the HCRI indicators contain a strong common multivariate structure at the global level. However, this result does not imply that global PCA is sufficient to represent the spatially varying structure of household resilience. Global PCA summarizes one overall covariance structure for all households, whereas household climate resilience may vary across locations owing to differences in exposure, housing conditions, health burden, economic capacity, and adaptation responses. Therefore, the global PCA result is treated as a baseline diagnostic rather than as the final HCRI model.

This covariance-based baseline is also consistent with the previously published robust global HCRI framework of Sundari *et al.* (2026). In that study, the HCRI was constructed from 221 household observations across 17 urban villages in Jakarta using four resilience dimensions: exposure, sensitivity, incremental adaptation, and transformational adaptation. The study applied Robust PCA with the MCD estimator to reduce the influence of outliers and obtain a stable component estimation. The published Robust PCA-MCD results showed that PC1 explained 87.38% of the total variance, supporting the use of PC1 as a dominant one-number summary of household resilience, while reducing the influence of atypical multivariate observations.

Based on this global evidence, a covariance-based specification was retained in the present study. This choice was not made to ignore the scale issue but to preserve meaningful magnitude differences among household resilience indicators after indicator orientation and transformation. Several HCRI indicators, such as distance to flood sources, number of flood days, house elevation, building area, land area, health-related proportions, and household expenditures, contain substantive magnitude information. Standardizing all the indicators would place all variables in equal variance but may also reduce the intended role of empirical magnitude differences in index construction. Therefore, the covariance-based approach was considered appropriate because the objective of this study was to extend the previously established robust covariance-based HCRI framework into a geographically weighted setting.

Therefore, the present Robust GWPCA-MCD model is positioned as a spatial extension of the robust global PCA-MCD framework, rather than as a separate index-construction logic. The global PCA baseline confirms that the HCRI indicators have a strong overall multivariate structure, whereas the local Robust GWPCA-MCD model examines whether this structure varies across household locations. This transition from a global to local analysis is important because urban household resilience in Jakarta is not expected to be spatially uniform. Local differences in flood exposure, housing sensitivity, water access, health burden, and adaptation capacity may produce different dominant indicators across neighborhoods.

However, the global PCA baseline was not used as the sole justification for the final HCRI. The covariance-based specification remains sensitive to indicator variance, and this limitation is acknowledged in the interpretation. For this reason, the following sections report additional local diagnostics, including adaptive bandwidth, local support, local PC1 variance, eigenvalue behavior, and top local PC1 loadings. These diagnostics were used to assess whether the local HCRI structure was sufficiently stable and interpretable, rather than relying only on the high global PC1 variance.

Table 5. Global PCA Baseline for HCRI Construction.

Method	Min (%)
PCA-SVD	87,46
PCA Kovarian	87,46
Robust PCA MCD	87.38

3.3. Robust Mahalanobis Distance and Multivariate Household Profiles

Before estimating the Robust GWPCA-MCD model, multivariate household profiles were examined using the robust Mahalanobis distance. This diagnostic step identified observations whose joint indicator patterns differed substantially from the central multivariate structure of the data. In multivariate analysis, the Mahalanobis distance is commonly used to measure the extent to which an observation lies from the multivariate center after accounting for the covariance structure among variables. However, because the classical mean vector and covariance matrix are sensitive to atypical observations, a robust version based on the MCD estimator is preferred when the data may contain multivariate outliers or high-leverage observations (Hubert & Rousseeuw, 2005; Rousseeuw, 1984; Rousseeuw & Driessen, 1999).

The robust Mahalanobis distance was calculated using a 13-variable numerical subset selected specifically for multivariate outlier diagnostics. Therefore, the value $p = 13$ refers only to the degrees of freedom used in the robust Mahalanobis distance cutoff, not to the full HCRI construction stage. This distinction is important because the final Robust GWPCA-MCD model used 30 HCRI indicators, whereas the outlier diagnostic was conducted on a narrower numerical subset to evaluate multivariate leverage before robust local covariance estimation.

The diagnostic result showed that 95 household observations exceeded the χ^2 (99%) cutoff value of 27.688 with $p = 13$, corresponding to 41.6% of households being flagged as multivariate outliers. This proportion is relatively high, indicating that the household resilience data contain substantial multivariate heterogeneity. Therefore, the flagged observations were not interpreted as simple data errors or marginal noise. Instead, they were treated as atypical household profiles that may reflect meaningful differences in exposure, housing conditions, health impacts, economic capacity, and adaptation behavior across the sampled urban villages.

This interpretation is consistent with the logic of robust PCA, in which outlier diagnostics are used not only to remove observations but also to justify the use of robust covariance estimation. Sundari *et al.* (2026) emphasized that flagged observations were not mechanically deleted; rather, outlier screening was used to motivate robust covariance estimation such that the component directions were not dominated by a minority of extreme multivariate profiles, while households remained available for scoring and spatial mapping. This principle is also relevant to the present study because household resilience data may contain atypical but substantively meaningful observations.

The high proportion of flagged observations provides an empirical justification for the use of a robust covariance estimator. Classical covariance-based PCA may be affected by high-leverage observations because a small number of atypical profiles can rotate the principal directions and influence the eigenvectors used to define component loadings (Hubert & Rousseeuw, 2005; Jolliffe, 2002). In the published HCRI study, this concern was also noted: classical covariance-based PCA can be rotated by leverage points that disproportionately affect the sample covariance matrix and the resulting eigenvectors. Therefore, MCD-based robust covariance estimation is appropriate for reducing the influence of such observations while preserving the multivariate structure of the data.

In the context of GWPCA, the outlier issue becomes more important because the covariance matrices are estimated locally. Unlike global PCA, which summarizes one covariance structure for all observations, GWPCA estimates local covariance structures using geographically weighted observations (Harris *et al.,* 2011). Consequently, an atypical household located within a local neighborhood may have a stronger influence on the local eigenvalues, eigenvectors, component loadings, and PC1 scores than it would in a global model. This condition strengthens the rationale for using Robust GWPCA-MCD, because the local covariance structure should be protected from excessive leverage while retaining meaningful household variation.

The robust Mahalanobis distance result suggests that household resilience in Jakarta is not represented by a single homogeneous profile. Some households may experience high exposure but possess stronger adaptive capacity, whereas others may face lower exposure but greater sensitivity or weaker coping resources. This variation is consistent with the multidimensional nature of household resilience, which combines exposure, sensitivity, and incremental and transformational adaptation. In the published HCRI framework, these four dimensions were used to construct a household-level resilience index for 221 respondents from 17 urban villages in Jakarta.

Thus, the robust Mahalanobis distance diagnostic serves as a bridge between the global PCA baseline and the local Robust GWPCA-MCD model. The diagnostic indicates that robust treatment is needed because the household data contain heterogeneous multivariate profiles, whereas the geographically weighted framework is needed because the structure of resilience may vary across locations. The robust Mahalanobis distance plot is shown in Figure 4. Observations above the χ^2 (99%) cutoff are interpreted as atypical multivariate household profiles that require robust covariance treatment, not as observations to be automatically excluded from the HCRI construction.

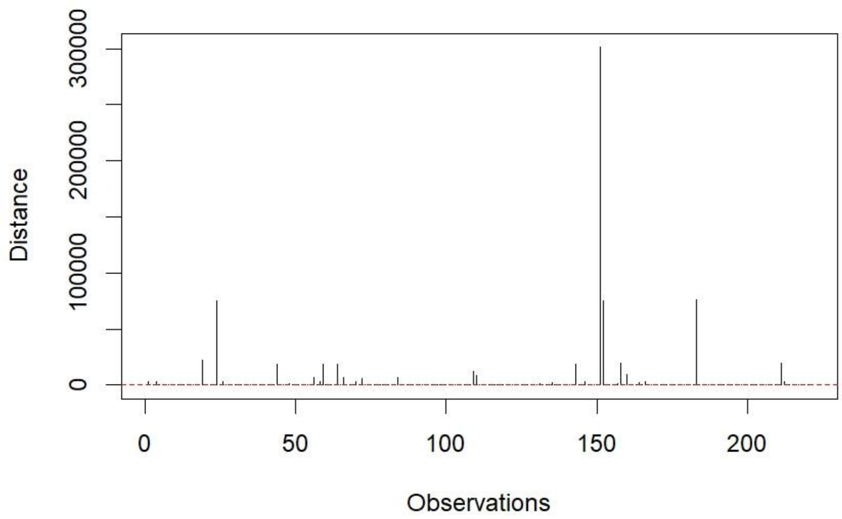

Figure 4. Robust Mahalanobis Distance.

3.4. Robust GWPCA-MCD Model Calibration and Local Support

After the global PCA baseline and robust Mahalanobis distance diagnostics, the local model was estimated using Robust GWPCA-MCD. This model was designed to extend the previously established robust covariance-based HCRI framework into a geographically weighted setting. The objective was not only to obtain a single global resilience gradient but also to examine whether the dominant multivariate structure of household resilience varied across household locations.

The final Robust GWPCA-MCD model was estimated using 221 household observations and 30 final HCRI indicators. Two components were retained in the model, and a bisquare kernel was used to construct the geographical weighting scheme. The selected bandwidth was adaptive, meaning that the local model was calibrated using a fixed number of nearest neighbors rather than a fixed geographical distance. The non-robust GWPCA model selected 120 nearest neighbors, whereas the Robust GWPCA-MCD model selected 96 nearest neighbors. The robust model used the MCD estimator with $\alpha = 0.75$, resulting in an approximate local h-subset of 72 observations.

The use of an adaptive bandwidth is important because household observations are not uniformly distributed across space. In geographically weighted analysis, adaptive bandwidth helps maintain a comparable number of observations around each target location, especially when the density of the sampled households varies across the study area. This is particularly relevant for local PCA, because each location requires a sufficiently supported local covariance matrix before eigenvalue decomposition can be performed. Therefore, the selected bandwidth reflects a balance between preserving local spatial variation and maintaining numerical stability in the covariance estimation.

In this study, the selected bandwidth of 96 nearest neighbors provides a local neighborhood size approximately 3.20 times the number of final HCRI indicators. With MCD $\alpha = 0.75$, the approximate robust h-subset is 72 observations, corresponding to 2.40 times the number of indicators. This indicates that the local covariance estimation was supported by a neighborhood size larger than the number of variables. Such local support is important because covariance estimation with a small neighborhood relative to the number of indicators may produce unstable eigenvalues, unstable loading directions, or nearly singular local covariance matrices.

The bisquare kernel assigns larger weights to observations closer to the target location and smaller weights to more distant observations, whereas observations outside the local bandwidth receive zero weight. In the diagnostic procedure, local support was assessed by calculating the number of non-zero-weighted neighbors and the effective local sample size for each location. The effective local sample size was computed from the concentration of geographical weights using the squared sum of weights divided by the sum of squared weights. This diagnostic was used to ensure that the local covariance structure was interpreted not only from the nominal bandwidth but also from the effective contribution of nearby observations.

The use of MCD-based robust covariance estimation further strengthens the local model calibration. The robust Mahalanobis distance diagnostic showed substantial multivariate heterogeneity in the household data; therefore, a classical local covariance matrix may be sensitive to atypical household profiles. In a geographically weighted setting, such profiles may exert a stronger influence because each local covariance matrix is estimated from a neighborhood subset rather than from the full dataset. By combining adaptive geographical weighting with MCD-based robust covariance estimation, Robust GWPCA-MCD mitigates the influence of high-leverage observations while retaining substantively meaningful household variation.

The retained two-component structure follows the general PCA principle that principal components summarize the main directions of variation in a multivariate dataset. Component loadings represent the contribution of indicators, whereas component scores represent the transformed positions of households in the component space. In the present study, PC1 was emphasized as the main local HCRI gradient, whereas PC2 was retained to evaluate additional local variation and cumulative local variance.

Overall, the model calibration results indicate that Robust GWPCA-MCD provides a locally supported framework for estimating spatially varying HCRI structures. However, the model is not interpreted solely based on bandwidth selection or high PC1 variance. The subsequent analysis also considers local PC1 variance, eigenvalue behavior, condition number, and dominant local loadings to evaluate whether the local HCRI structure is stable and substantively interpretable.

Table 6. Robust GWPCA-MCD Model Settings.

Calibration aspect	Setting
Geographical kernel	Bisquare
Bandwidth type	Adaptive nearest neighbors
Selected bandwidth	96 neighbors
Robust covariance estimator	MCD
MCD tuning parameter	$\alpha = 0.75$
Approximate local h-subset	72 observations
Bandwidth-to-variable ratio	3.20
h-subset-to-variable ratio	2.40
Scale specification	Original/covariance-based

3.5. Comparison of Classical GWPCA and Robust GWPCA-MCD: Local PC1 Variance and Information Sufficiency

After calibrating the Robust GWPCA-MCD model, the local variance explained by the first principal component was evaluated and compared with the classical GWPCA results. This comparison was made to assess whether the robust local covariance specification produced a more informative local PC1 structure than the non-robust covariance-based GWPCA. In PCA, the first principal component represents the dominant linear combination of the original indicators, whereas the proportion of variance explained by PC1 reflects the amount of multivariate information summarized by this component (Jolliffe, 2002; Jolliffe & Cadima, 2016). In the HCRI framework, this diagnostic is important because PC1 scores are used as the basis for constructing household resilience scores, whereas component loadings represent the contribution of indicators to the resilience gradient.

The comparison shows a clear difference between the classical and robust GWPCA-MCD results. The classical GWPCA model, using an adaptive bandwidth of 120 nearest neighbors, produced a local PC1 variance ranging from 12.35% to 79.17%, with a median of only 14.81%. In contrast, the Robust GWPCA-MCD model, using an adaptive bandwidth of 96 nearest neighbors, produced a local PC1 variance ranging from 63.42% to 99.999%, with a median of 83.66%. This indicates that the first component in the classical GWPCA model did not consistently summarize the local covariance structure, whereas the robust model produced a substantially stronger local PC1 structure across household locations.

Table 7. Comparison between Classical GWPCA and Robust GWPCA-MCD.

Method	Min (%)	Q1(%)	Q2(%)	Q3(%)	Max (%)
GWPCA	12,347	13,762	14,807	16,828	79,174
Robust GWPCA MCD	63,424	78,094	83,655	85,535	99,999

The low median local PC1 variance in the classical GWPCA results suggests that the local covariance structure was fragmented across several components. In other words, the first component alone was not sufficiently dominant in many local neighborhoods. This condition may occur when the local covariance estimation is affected by heterogeneous household profiles, high-leverage observations, or uneven spatial variation in the indicators. As household resilience indicators combine exposure, sensitivity, health burden, housing characteristics, economic capacity, and adaptation responses, the local covariance structure may be difficult to summarize using a single non-robust principal component.

The Robust GWPCA-MCD results provide stronger evidence for information sufficiency. The robust model produced a local PC1 variance with a minimum of 63.42%, Q1 of 78.09%, a median of 83.66%, Q3 of 85.54%, and a maximum of 99.999%. A median value above 80% indicated that, for most household locations, PC1 captured a large proportion of the local multivariate variation. This finding supports the use of PC1 as the main local HCRI gradient. This result is consistent with the applied PCA criterion that components explaining a substantial proportion of the total variance can be retained for interpretation, with 70% often used as a practical benchmark in index construction.

However, the high local PC1 variance should not be interpreted mechanically. The minimum value of 63.42% indicates that some local neighborhoods still had more complex multivariate structures, whereas PC1 did not capture as much variation as in other locations. Conversely, the maximum value of 99.999% indicates a nearly complete concentration of local variance in PC1. This may reflect a strongly dominant local component but may also indicate a highly concentrated local covariance structure. Therefore, local PC1 variance must be interpreted together with model calibration, bandwidth sensitivity, local support, and loading stability, rather than as a standalone measure of model quality.

Bandwidth sensitivity was then evaluated to examine whether the robust local PC1 structure remained stable under neighboring bandwidth alternatives. The main Robust GWPCA-MCD bandwidth was 96 nearest neighbors. When the bandwidth was reduced to 86, the median local PC1 variance remained high at 80.86%, with 91.86% agreement for top-ranked loading and 85.97% agreement for the HCRI classification. When the bandwidth was increased to 106 and 120, the median local PC1 variance increased slightly, but the HCRI class agreement declined to 61.09% and 44.80%.

The sensitivity results indicated that a higher local PC1 variance did not automatically imply a better local model. Although larger bandwidths produced slightly higher median LPV PC1, they reduced agreement in both the dominant loading and the HCRI classification. This pattern suggests that wider bandwidths may smooth the local differences too strongly, thereby weakening the spatial specificity of the HCRI classification. Therefore, the selected bandwidth of 96 nearest neighbors provides a practical balance between variance explanation, loading stability, and local interpretability.

Table 8. Bandwidth Sensitivity of Robust GWPCA-MCD.

Bandwidth	LPV PC1 median (%)	Top-1 loading agreement (%)	HCRI class agreement (%)
86	80.86	91.86	85.97
96	83.66	100.00	100.00
106	84.42	81.90	61.09
120	84.91	69.68	44.80

Overall, the comparison between classical GWPCA and Robust GWPCA-MCD supports the use of the robust local covariance approach. Classical GWPCA produced a low median local PC1 variance, indicating that PC1 was not consistently informative across locations. Robust GWPCA-MCD produced a stronger and more stable PC1 structure while retaining spatial variation in household resilience. Therefore, PC1 from the Robust GWPCA-MCD model was used as the main local HCRI gradient in the subsequent scoring and classification stage.

3.6 HCRI Score Distribution and Classification Results

Following the scoring and classification procedure described in Section 2.6, the aligned local PC1 scores obtained from the Robust GWPCA-MCD were transformed into HCRI classes. This section presents the empirical classification thresholds and the resulting distribution of households across the resilience categories. Consequently, emphasis is placed on the observed resilience structure rather than on the classification procedure.

The empirical HCRI thresholds are presented in Table 9. Based on the aligned local PC1 scores, the first quartile (Q1), median (Q2), and third quartile (Q3) are 0.7390, 0.7690, and 1.2200, respectively. The corresponding lower and upper boxplot fences are 0.0175 and 1.9415, respectively. These empirical thresholds were subsequently used to classify households into six ordered resilience categories ranging from Extremely Low to Extremely High.

Table 9. Empirical Thresholds for HCRI Classification.

Threshold	Value
Lower fence	0.0175
Q1	0.7390
Median (Q2)	0.7690
Q3	1.2200
Upper fence	1.9415
Threshold	Value

The resulting HCRI class distribution is presented in Table 10. The largest proportion of households belonged to the high resilience class (58 households; 26.24%), followed by the very high resilience class (56 households; 25.34%). Meanwhile, 52 households (23.53%) were classified as low, 12 (5.43%) as very low, and 43 (19.46%) as extremely low. None of the households were classified as extremely high, indicating that none of the aligned local PC1 scores exceeded the upper classification boundary.

Table 10. Distribution of Households by HCRI Class.

HCRI Class	Frequency	Percentage (%)
Extremely Low	43	19.46
Very Low	12	5.43
Low	52	23.53
High	58	26.24
Very High	56	25.34
Extremely High	0	0.00

The class distribution indicates that household resilience was heterogeneous across the study area. Slightly more than half of the sampled households (51.58%) were classified into the High and Very High resilience categories, suggesting that many households possessed relatively stronger resilience profiles within the observed sample. Nevertheless, nearly one-fifth of the households (19.46%) were classified as Extremely Low, indicating the presence of a vulnerable subgroup with substantially weaker multivariate resilience characteristics.

The absence of households in the Extremely High category suggests that although several households demonstrated relatively strong resilience, none exhibited resilience scores sufficiently distant from the upper empirical boundary to be considered statistically extreme. Conversely, the relatively large Extremely Low group reflects a pronounced lower tail in the HCRI distribution, highlighting households that may require greater policy attention and more targeted climate adaptation interventions.

The HCRI classification provides a concise summary of household resilience conditions before considering their geographical contexts. Although Table 10 describes the overall distribution of resilience classes, it does not reveal where these households are located. Therefore, the following section examines the spatial distribution of the HCRI categories to identify whether lower- and higher-resilience households exhibit distinct geographical clustering across the sampled urban villages.

3.7. Spatial Distribution of HCRI Categories

The classification of the HCRI across selected urban villages reveals clear contrasts among administrative areas and forms a pattern that may be described as a "dual pattern." This pattern refers to the coexistence of locations that, despite high hazard exposure, remain in high resilience classes alongside other locations with similar exposure levels that are instead concentrated in low-resilience categories. This finding confirms that household resilience is not determined solely by disaster exposure but emerges from the interaction between exposure, adaptive capacity, and enabling conditions, such as access to basic services, infrastructure quality, and local social–institutional support (Cutter *et al.,* 2008; Meerow *et al.,* 2016; Norris *et al.,* 2008). Thus, the spatial distribution of HCRI categories not only identifies "where risks are located" but also reveals "where capacities are able to offset those risks."

Central Jakarta appears to be the most consistently resilient. Kampung Bali and Karet Tengsin each recorded 100.00% of households in the Very High Resilience category, despite differing vulnerability profiles (Kampung Bali: high vulnerability to drought hazards; Karet Tengsin: low vulnerability to flood hazards). West Jakarta exhibited strong polarization: Duri Selatan (moderate vulnerability, drought, and extreme heat) was dominated by the High category (92.31%), with a small share of Very High (7.69%), whereas Krendang (moderate vulnerability, extreme heat) was entirely High (100.00%). In contrast, highly vulnerable villages in the same municipality were concentrated in the lowest resilience classes: Kamal (flood, tidal flood, and extreme heat) was distributed across Very Low (15.38%) and Extremely Low (84.62%) Resilience, and Semanan (flood, extreme heat) was Extremely Low (100.00%).

South Jakarta also displayed sharp heterogeneity. Cilandak Timur (high vulnerability: flood, drought, and extreme heat) and Ragunan (extremely low vulnerability) both recorded 100.00% in the Very High category, whereas North Petukangan (high vulnerability: flood and extreme heat) was Extremely Low (100.00%). Ulujami (low vulnerability: extreme heat) showed a more layered distribution: Very High (23.08%), High (7.69%), Very Low (23.08%), and Extremely Low (46.15%), indicating internal inequality of resilience within the same village.

In East Jakarta, villages with extremely high vulnerability tend to cluster in the lower classes. Jatinegara (extremely high vulnerability; flood) was dominated by Low (92.31%) and Very Low (7.69%) vulnerability, while Malaka Jaya (Very Low vulnerability) was dominated by Very Low vulnerability (92.30%) and Extremely Low vulnerability (7.69%). Rawa Terate (very high vulnerability; flood and drought) was split between High (53.85%) and Low (46.15%) vulnerability, suggesting that exposure and resilience may coexist in nonlinear ways.

In North Jakarta, the influence of coastal hazards remained heterogeneous. Koja (very high vulnerability: flood, drought, and tidal flood) was dominated by High (76.92%) and Very Low vulnerability (23.08%), while Marunda (very high vulnerability: drought and tidal flood) was dominated by Low (92.31%) and Very Low (7.69%) vulnerability. Pluit (low vulnerability: tidal flood) was dominated by Low (76.92%), High (15.38%), and Very Low vulnerability (7.69%). Interestingly, Tanjung Priok (very high vulnerability: flood and tidal flood) showed 100.00% High, reinforcing the "dual pattern": high exposure does not necessarily imply low resilience.

These inter-village variations confirm the relevance of a place-based approach for policy formulation. Strategies to enhance resilience must be tailored to the specific combination of risk and capacity at each location. Villages concentrated in the lowest classes (e.g., Kamal, Semanan, and North Petukangan) require prioritized investment in basic services, protective infrastructure, and household-level adaptive support. Conversely, villages that remain resilient under high exposure (e.g., Tanjung Priok and several Central Jakarta cases) can be treated as positive deviance sites to extract effective practices and enabling conditions that may be adapted and replicated elsewhere (Meerow *et al.,* 2016; Norris *et al.,* 2008).

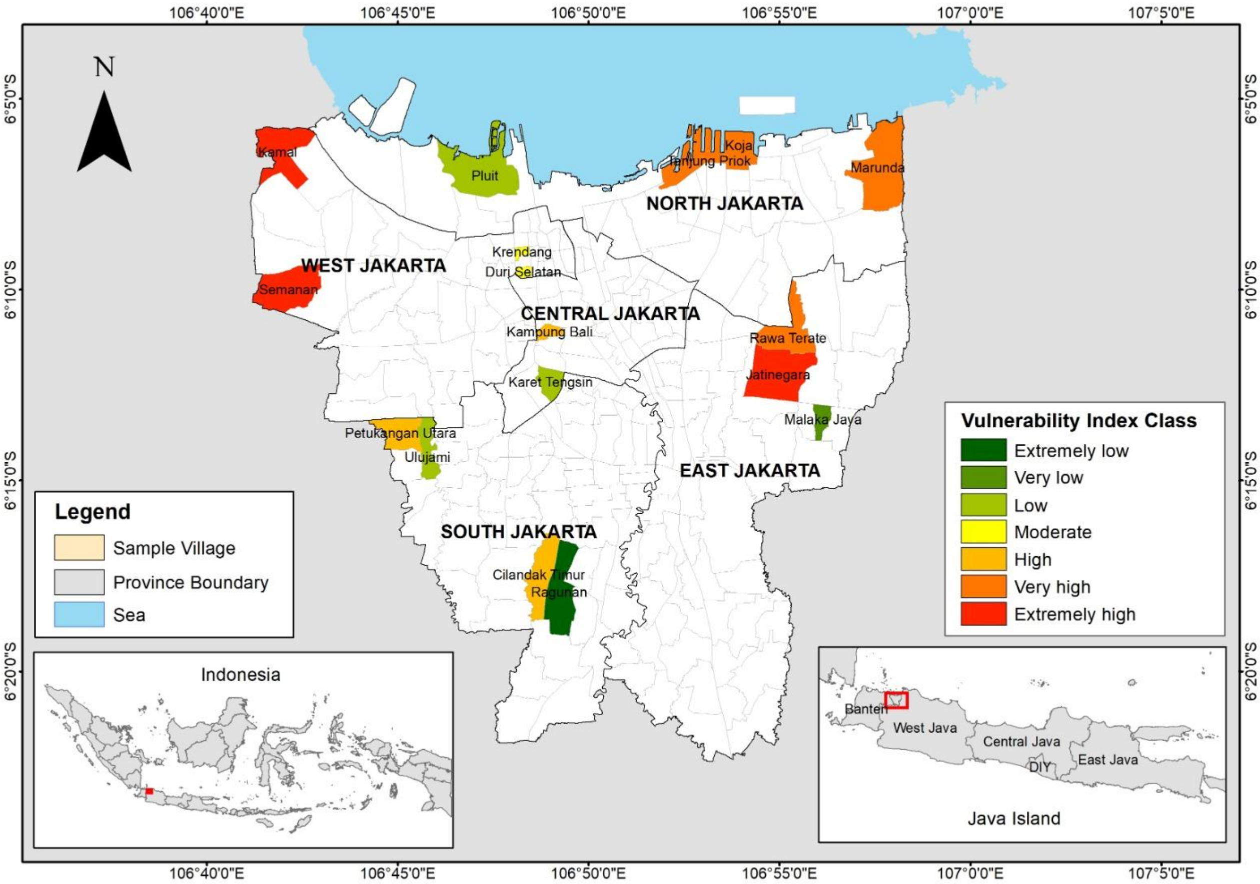

Figure 5. Vulnerability Index Class.

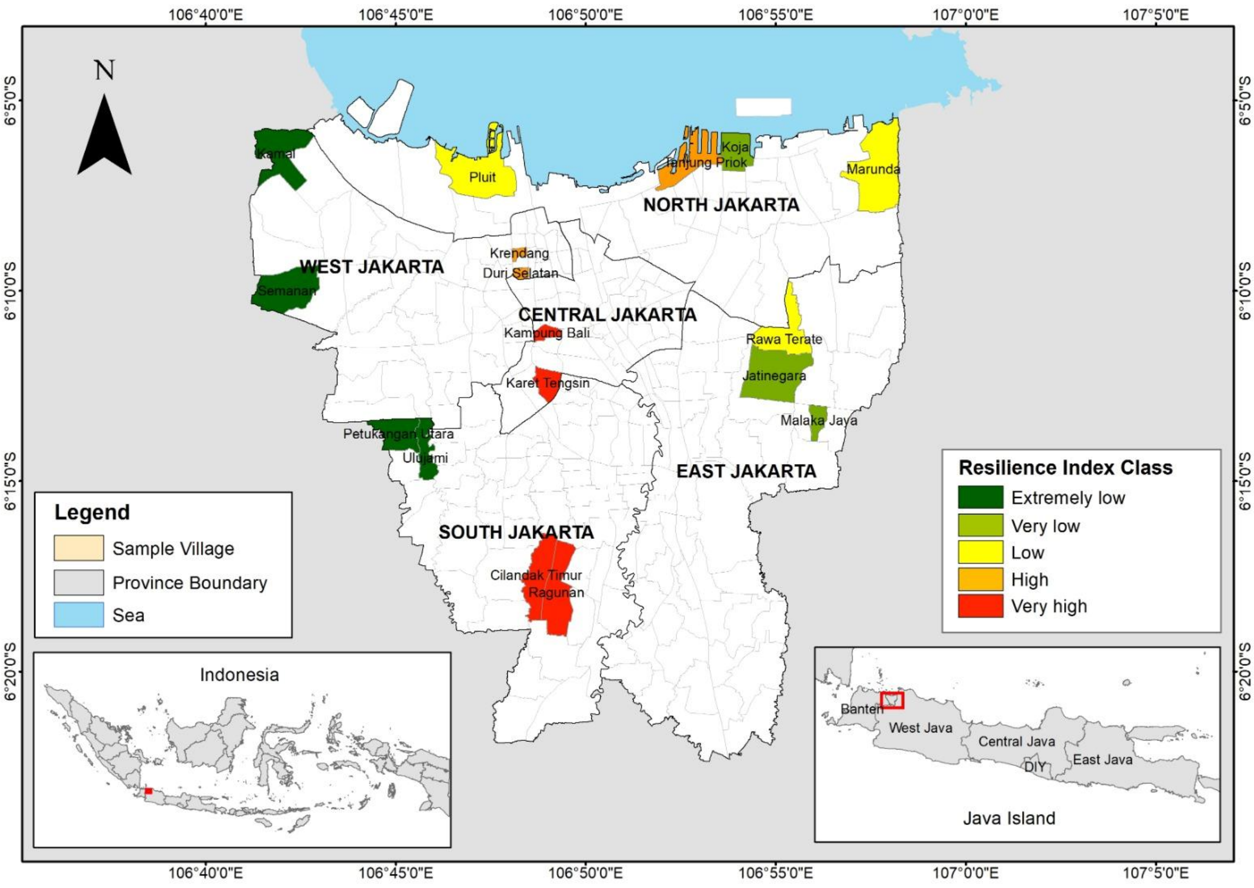

Figure 6. Resilience Index Class.

3.8. Local Dominant Indicators Based on PC1 Loadings

After examining the spatial distribution of the HCRI categories, the local PC1 loadings were analyzed to identify the indicators that contributed most strongly to the Robust GWPCA-MCD-based HCRI structure at each location. While Section 3.7 shows where lower and higher resilience categories are located, this section explains which indicators form the dominant local resilience gradient. In the PCA-based index construction, component loadings represent the contribution of the indicators to the principal component, whereas component scores represent household positions in the component space.

The dominant local indicator was identified from the variable with the largest absolute aligned loading on PC1. The use of aligned loadings was important because the direction of PC1 was adjusted so that higher PC1 scores consistently represented higher resilience. In the diagnostic output, the top local loadings were reported together with the aligned loading values, absolute aligned loadings, and loading signs. The full output also stored the top three loadings for the Robust GWPCA-MCD and classical GWPCA as separate diagnostic sheets, allowing comparison between robust and non-robust local loading structures.

The results showed that the dominant local indicators were not uniform across the sampled urban villages. Several locations were dominated by exposure indicators, particularly C3b and C2b, which represented distance to flood sources. C3b measures the distance to other flood sources, whereas C2b measures the distance of the house to the main flood source. Other locations were dominated by the sensitivity indicators, particularly B3, B4, E14, and I5. B3 and B4 represent building and land areas, whereas E14 and I5 represent medication expenditure and the proportion of sick family members after the drought.

The local loading structure indicates that household resilience in Jakarta is mainly shaped by two dominant dimensions: exposure and sensitivity. Exposure-dominant areas include Jatinegara, Koja, Malaka Jaya, Marunda, Rawa Terate, and Tanjung Priok. In these locations, the local HCRI gradient is primarily associated with proximity to flood-related hazard sources. This suggests that the spatial position of households relative to flood sources is an important component of local resilience differentiation.

Sensitivity-dominant areas include Cilandak Timur, Duri Selatan, Kamal, Kampung Bali, Karet Tengsin, Krendang, Petukangan Utara, Pluit, Ragunan, Semanan, and Ulujami. At these locations, the dominant PC1 loadings were mainly associated with housing characteristics, land or building areas, medication expenditures, and health-related drought impacts. This pattern suggests that household resilience in these areas is more strongly differentiated by internal household conditions and post-hazard burden than by exposure distance alone.

At the household level, the most frequent dominant indicator was C3b, followed by B3, B4, E14, C2b, and I5. This distribution confirms that the local HCRI structure was not driven by a single indicator across the entire study area. Instead, different indicators became dominant in different local contexts. The presence of C2b and C3b as dominant indicators highlights the importance of flood-source proximity, whereas the dominance of B3 and B4 indicates the role of housing and settlement characteristics. Meanwhile, E14 and I5 show that health and post-disaster burdens also contribute to local differences in resilience.

The spatial visualization in Figure 7 provides a local interpretation of the Robust GWPCA-MCD results. Areas dominated by exposure indicators indicate locations where household resilience is primarily structured by spatial hazard proximity. Areas dominated by sensitivity indicators indicate locations where resilience differences are more closely related to household internal conditions, such as housing characteristics, health burdens, and economic consequences after climate-related events.

The dominance of the sensitivity indicators in many urban villages is important. It implies that household resilience is determined not only by whether households are located near or far from hazard sources but also by their capacity to absorb and manage climate-related impacts. In this sense, Robust GWPCA-MCD provides more than a spatial classification of resilience levels; it also identifies the local indicator structure underlying these resilience categories.

Overall, the local dominant loading analysis supports the main argument that household climate resilience is spatially heterogeneous. Different urban villages are characterized by different dominant indicators, indicating that adaptation priorities should not be generalized across all locations. Exposure-dominant areas may require interventions related to flood-risk reduction, drainage improvement, or spatial hazard management, whereas sensitivity-dominant areas may require attention to housing conditions, health protection, water access, and household recovery capacity. This interpretation provides the basis for linking the HCRI results to location-specific adaptation planning.

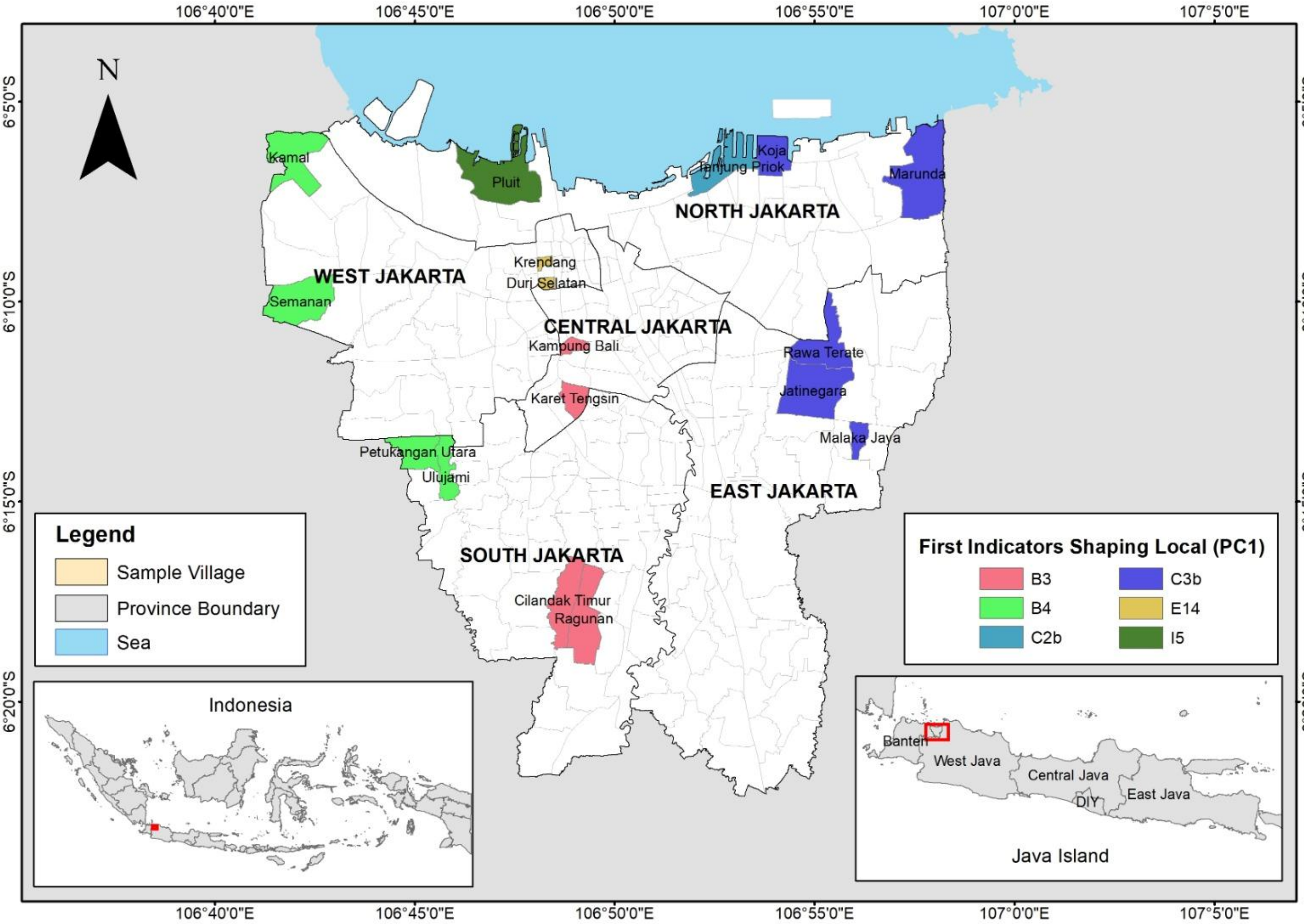

Figure 7. First indicators shaping local PC1.

3.9. Robustness and Sensitivity Summary

Robustness and sensitivity diagnostics were used to evaluate whether the Robust GWPCA-MCD-based HCRI was statistically stable and substantively interpretable. These diagnostics were not intended to introduce a new model but to support the reliability of the selected local HCRI specifications. The assessment focused on three aspects: bandwidth sensitivity, classification stability, and consistency of the covariance-based robust specification.

The bandwidth sensitivity results showed that the selected bandwidth of 96 nearest neighbors provided the most balanced specification. At this bandwidth, the median local PC1 variance was 83.66%, with 100% agreement in both the top-ranked local loading and the HCRI class relative to the main model. When the bandwidth was reduced to 86 neighbors, the model still produced a high median local PC1 variance of 80.86%, with 91.86% top-1 loading agreement and 85.97% HCRI class agreement. However, when the bandwidth was increased to 106 and 120 neighbors, the HCRI class agreement declined substantially to 61.09% and 44.80%, respectively.

This pattern indicates that higher local PC1 variance alone is insufficient to determine the best local model. Although wider bandwidths produced a slightly higher median local PC1 variance, they reduced the consistency of the HCRI classes and dominant loading patterns. This suggests that excessive spatial smoothing may weaken the local specificity of household resilience structures. Therefore, the selected bandwidth of 96 nearest neighbors was retained because it provided a balance between local variance explanation, loading stability, and HCRI classification consistency.

The classification stability diagnostic was also used to evaluate whether the final HCRI categories were sensitive to the classification rule. The main classification was based on quartile cutoffs and boxplot fences, whereas equal-interval and six-quantile classifications were computed as sensitivity alternatives. The output stored the main box-fence, equal-interval, and quantile-based classes for each household, allowing us to examine the stability of the resulting HCRI categories. This step is important because the PCA-based index classes are relatively empirical categories that depend on the observed score distribution rather than absolute resilience thresholds.

The covariance-based specification was also examined using a scale-related diagnostic. The main Robust GWPCA-MCD model used the original covariance-based scale, and a standardized/correlation-based diagnostic was generated for comparison. In the available output, both specifications produced the same bandwidth of 96 nearest neighbors, the same local PC1 variance summary, and 100% agreement in both the top-ranked loading and HCRI class. This result suggests that the main HCRI pattern was not altered by the standardized diagnostic in the implemented analysis. Nevertheless, the covariance-based specification remained the main model because this study aimed to preserve meaningful magnitude differences among household indicators after orientation and transformation.

Taken together, these diagnostics support the use of Robust GWPCA-MCD as the final local HCRI model. The bandwidth sensitivity results show that the selected bandwidth preserves local interpretability better than wider neighborhoods. The classification diagnostic confirms that the HCRI classes were evaluated against the alternative grouping rules. The scale-related diagnostic indicates that the main covariance-based HCRI pattern remained consistent under the standardized comparison. Thus, the final HCRI was justified not only by a high local PC1 variance but also by supporting diagnostics related to bandwidth, loading agreement, classification consistency, and scale sensitivity.

Overall, the robustness and sensitivity results strengthened the empirical basis of the Robust GWPCA-MCD-based HCRI. The final model captures spatial heterogeneity in household climate resilience while mitigating the influence of high-leverage multivariate observations through robust local covariance estimation. Therefore, the resulting HCRI classes and local dominant indicators can be interpreted as spatially specific household resilience profiles, rather than as artifacts of a single global covariance structure, arbitrary bandwidth selection, or a single classification rule.

4. Discussion

The results demonstrate that Robust GWPCA-MCD provides a more informative and interpretable framework for constructing a local HCRI than classical GWPCA. Comparison between classical GWPCA and Robust GWPCA-MCD showed that the non-robust model produced a weak local PC1 structure, with a median local PC1 variance of only 14.81%. In contrast, Robust GWPCA-MCD produced a substantially stronger local PC1 structure, with a median local PC1 variance of 83.66%. This improvement indicates that the robust local covariance estimator could extract a more coherent dominant resilience gradient from heterogeneous household data. This finding is consistent with the theoretical role of PCA as a dimension -reduction method that summarizes dominant multivariate variation through principal components (Jolliffe, 2002; Jolliffe & Cadima, 2016). However, in this study, local and robust extension is essential because household resilience is not only multivariate but also spatially heterogeneous and potentially influenced by high-leverage observations (Lu *et al.,* 2025; Tsutsumida *et al.,* 2022).

The advantage of Robust GWPCA-MCD is particularly important because the household resilience data contain substantial multivariate heterogeneity. The robust Mahalanobis distance diagnostic showed that a considerable proportion of households had atypical multivariate profiles, indicating that extreme observations were not merely isolated data errors but were part of the empirical structure of household resilience. In this context, classical covariance-based PCA or GWPCA may be sensitive to leverage points because the sample covariance matrix can be disproportionately affected by atypical observations. The MCD estimator was developed to provide robust estimates of multivariate location and scatter, making it appropriate for data structures in which outlying observations may rotate in the principal directions (Rousseeuw, 1984; Rousseeuw & Van Driessen, 1999; Hubert *et al.,* 2018 ; Li *et al.,* 2024). The implemented diagnostics also support this interpretation: Robust GWPCA-MCD retained a high local PC1 variance while maintaining stronger loading and classification stability than the non-robust GWPCA specification. This result is consistent with recent developments in robust multivariate analysis that continue to emphasize resistant covariance estimation when data contain atypical or high-leverage observations (Li *et al.,* 2024; Roy *et al.,* 2024).

The spatial results confirm that household climate resilience in Jakarta is not spatially uniform. The HCRI categories varied across the sampled urban villages, with some areas showing stronger resilience profiles and others dominated by lower-resilience categories. This supports the use of a geographically weighted approach because a single global covariance structure is insufficient to represent local variation in exposure, sensitivity, and adaptation capacity. The GWPCA was originally proposed to allow principal component structures to vary geographically, making it suitable for identifying local multivariate patterns that may be hidden in global PCA PCA (Harris *et al.,* 2011; Lu *et al.,* 2025; Tsutsumida *et al.,* 2022). The present study extends this logic by incorporating MCD-based robust covariance estimation so that local principal components are less influenced by atypical household profiles while still capturing spatial variation in the resilience structure. This spatially differentiated interpretation is also consistent with recent urban resilience studies emphasizing that resilience conditions and their underlying drivers vary substantially across locations (Sharifi, 2023; Suárez *et al.,* 2024).

The classification results further show that the HCRI distribution has an important lower-tail pattern. Although slightly more than half of the households were classified into the High and Very High categories, 43 households (19.46 %) were classified as Extremely Low. This indicates that a vulnerable subgroup exists in the empirical distribution of household resilience. The absence of an Extremely High class suggests that the upper tail of the HCRI distribution was less pronounced than the lower tail. Thus, the strongest resilience profiles in the sample remained within the non-extreme range, whereas the weakest profiles were sufficiently distant from the lower empirical boundary to form a distinct extreme group. This result is important for policy interpretation because resilience categories should be read not only as statistical labels but also as a tool to identify households and locations requiring differentiated adaptation attention. Recent index-based resilience studies similarly emphasize the usefulness of multidimensional indices for distinguishing heterogeneous resilience conditions and supporting targeted interventions across populations and locations (Fajardo-Gonzalez *et al.,* 2025; Pécsinger *et al.,* 2025; Suárez *et al.,* 2024).

The local loading analysis provides additional insights into why resilience differs across locations. The dominant local indicators were not uniform across the study area. Some urban villages were dominated by exposure indicators, especially distance to flood sources, whereas others were dominated by sensitivity indicators, such as building area, land area, medication expenditure, and post-drought health burden. This result shows that the lower or higher resilience categories are produced by different local mechanisms. In exposure-dominant areas, household resilience is mainly structured by proximity to hazard sources. In sensitivity-dominant areas, resilience is more strongly associated with internal household conditions, housing characteristics, and health and economic burdens after climate-related disturbances. This distinction is important because it prevents interpretation of the HCRI as a single-cause ranking. Instead, the index represents a spatially varying multivariate syndrome of household conditions. This interpretation is consistent with recent resilience-index applications showing that resilience emerges from multiple interacting dimensions whose relative importance varies across systems and local contexts (Albore *et al.,* 2025; Mafi-Gholami *et al.,* 2026; Singh *et al.,* 2025).

From a climate adaptation perspective, these findings align with the view that urban climate risk is shaped by the interaction between physical hazards, social vulnerability, infrastructure, and adaptive capacity. The IPCC AR6 Working Group II report emphasizes that climate impacts and adaptation capacity vary across human communities and that cities, settlements, and key infrastructures require context-specific adaptation options (IPCC, 2022; Lee *et al.,* 2023). Recent urban resilience literature similarly emphasizes interactions among social, ecological, technological, and infrastructural systems in shaping urban responses to climate stress (McPhearson *et al.,* 2022; Sharifi, 2023; Townend *et al.,* 2024). The same report also identifies coastal cities and settlements as specific contexts in which climate risks, vulnerability, and adaptation options require focused assessment. In Jakarta, this means that household resilience cannot be strengthened by household-level interventions alone. Adaptation also depends on broader urban systems, including drainage performance, flood control, water access, health services, housing quality, and land-use management. This is particularly relevant in Jakarta because recent evidence confirms that land subsidence and related physical risks remain spatially heterogeneous across the metropolitan area (Harintaka *et al.,* 2024).

The results of this study have direct implications for local adaptation planning. Areas dominated by exposure indicators require interventions that reduce hazard contact, such as improved drainage, flood-source management, coastal and riverine protection, and spatial planning, and exposure to recurrent inundation. Recent evidence on nature-based solutions indicates that flood- and heat-risk reduction is most effective when interventions are adapted to local conditions and integrated with broader urban resilience strategies (Ferrario *et al.,* 2024; Mosisa *et al.,* 2025). Areas dominated by sensitivity indicators require different interventions, including housing improvement, health protection, post-disaster support, water access, and household recovery assistance. Thus, the Robust GWPCA-MCD-based HCRI can support spatially differentiated adaptation planning by identifying not only areas with lower resilience but also the indicators that dominate the local resilience structure. This is consistent with the broader principle of climate-resilient development, in which adaptation combines household capacity, infrastructure, governance, and locally specific risk-reduction pathways (Schipper *et al.,* 2022; Sharifi, 2023; Townend *et al.,* 2024).

Methodologically, this study contributes to the literature by integrating robust covariance estimation into a geographically weighted PCA framework to construct a household resilience index. Previous HCRI research based on robust PCA-MCD provided a global robust index for Jakarta households; however, the present analysis extends this approach by allowing the covariance structure, PC1 variance, scores, and loadings to vary locally. The published HCRI framework used 221 mainland household observations across 17 urban villages and applied robust PCA with MCD to reduce the influence of outliers in global index construction. The current Robust GWPCA-MCD model builds on this foundation by adding a spatially local structure, thereby making the index more suitable for identifying geographically differentiated resilience profiles (Lu *et al.,* 2025; Tsutsumida *et al.,* 2022). Accordingly, the contribution of Robust GWPCA-MCD lies not merely in increasing local PC1 variance, but in combining robust covariance estimation with geographically varying multivariate structures to improve local interpretability.

The sensitivity diagnostics strengthen this methodological contribution. The selected bandwidth of 96 nearest neighbors provided a balance between local variance explanation, loading agreement, and HCRI class agreement. Wider bandwidths slightly increased the median local PC1 variance but substantially reduced classification agreement, indicating that excessive spatial smoothing can weaken local interpretability. The standardized diagnostic also showed that the main covariance-based robust HCRI pattern was not altered under the implemented standardized comparison, with 100% agreement in top-ranked loading and HCRI class.This finding is consistent with recent GWPCA research showing that local principal-component structures can be sensitive to bandwidth and geographical weighting specifications, making sensitivity evaluation important for reliable spatial interpretation (Lu *et al.,* 2025; Tsutsumida *et al.,* 2022). These findings support the claim that the final HCRI result was not only based on a high PC1 variance but was also evaluated through bandwidth, classification, loading, and scale-related diagnostics.

Despite these contributions, this study has several limitations. First, the analysis was based on 221 mainland household observations from 17 sampled urban villages; therefore, the findings should be interpreted as representing the sampled mainland Jakarta context rather than all the households in DKI Jakarta. Second, the HCRI classes are relatively empirical categories based on the observed distribution of aligned local PC1 scores; therefore, they should not be interpreted as absolutely safe or unsafe thresholds. This limitation is particularly relevant for multidimensional resilience indices, which are primarily intended to support comparative assessment and prioritization rather than define universal resilience thresholds (Fajardo-Gonzalez *et al.,* 2025; Suárez *et al.,* 2024). Third, the covariance-based specification was retained to preserve meaningful magnitude differences among the indicators; however, this also means that the model remains sensitive to the variance structure of the input variables. Fourth, the local dominant indicators should be interpreted as statistical contributors to the local PC1 structure, not as causal determinants. Future research should extend this framework by comparing the MCD and MRCD covariance estimators in more detail, incorporating longitudinal household resilience data, and testing whether local HCRI patterns remain stable under alternative sampling designs, kernels, and spatial scales.

Overall, the discussion shows that Robust GWPCA-MCD provides a statistically robust and spatially interpretable framework for household climate resilience assessment. The model improved the local information content of PC1, reduced the influence of high-leverage multivariate observations, and identified spatially varying dominant indicators. The results confirmed that household resilience in Jakarta is shaped by different combinations of exposure and sensitivity across locations. This finding is consistent with contemporary resilience research emphasizing that resilience is context-dependent, multidimensional, and spatially differentiated (Mafi-Gholami *et al.,* 2026; Sharifi, 2023; Suárez *et al.,* 2024; Townend *et al.,* 2024). Therefore, the proposed HCRI framework supports more targeted urban climate adaptation by linking local resilience classes with the specific indicators of structure vulnerability and adaptive capacity in each area.

5. Conclusion

This study developed a local HCRI for DKI Jakarta using Robust GWPCA-MCD. This method was applied to 221 mainland household observations and 30 final HCRI indicators representing exposure, sensitivity, incremental adaptation, and transformational adaptation. The results showed that Robust GWPCA-MCD produced a more informative local index structure than classical GWPCA. While classical GWPCA generated a low median local PC1 variance of 14.81%, Robust GWPCA-MCD increased the median local PC1 variance to 83.66%. This indicates that the robust local covariance estimation improved the ability of PC1 to summarize the dominant multivariate structure of household resilience across locations.

The final Robust GWPCA-MCD model used an adaptive bisquare kernel with 96 nearest neighbors, MCD $\alpha = 0.75$, and an approximate robust local h-subset of 72 observations. The bandwidth sensitivity diagnostics showed that this specification provided a balance between local variance explanation, loading agreement, and HCRI class stability. Wider bandwidths slightly increased the median local PC1 variance but reduced HCRI class agreement, indicating that excessive spatial smoothing may weaken the local interpretation of household resilience. Therefore, the selected Robust GWPCA-MCD specification was retained as the final local HCRI model.

The HCRI classification results showed that household resilience was heterogeneous across the study area. The largest share of households was classified as high resilience (26.24%), followed by very high resilience (25.34%), low resilience (23.53%), extremely low resilience (19.46%), and very low resilience (5.43%). No households were classified as extremely high. The existence of 43 households in the extremely low category indicates the presence of a vulnerable lower-tail group whose multivariate resilience profile deviates substantially from the central distribution. This group requires further attention in terms of spatial interpretation and adaptation planning.

The spatial distribution of the HCRI categories confirms that household resilience in Jakarta is not geographically uniform. Lower- and higher-resilience classes were concentrated in different sampled urban villages, supporting the use of a geographically weighted approach. The local dominant loading analysis further showed that the HCRI structure was shaped by different indicators across locations. Some areas were dominated by exposure indicators, particularly distance to flood sources, whereas other areas were dominated by sensitivity indicators, such as building area, land area, medication expenditure, and post-drought health burden. This result demonstrates that household resilience should not be interpreted as a single homogeneous construct across Jakarta but as a spatially varying multivariate condition.

Overall, Robust GWPCA-MCD provides a robust and spatially interpretable framework for constructing an HCRI. This method reduces the influence of high-leverage multivariate observations, improves the local information content of PC1, and identifies spatially specific dominant indicators. From a policy perspective, the results suggest that climate adaptation interventions should be differentiated locally. Exposure-dominant areas require interventions related to flood-risk reduction and spatial hazard management, whereas sensitivity-dominant areas require interventions related to housing conditions, health protection, water access, and household recovery capacity. Future research should extend this framework by comparing the MCD- and MRCD-based local covariance estimators, testing alternative kernels and bandwidths, and applying the model to longitudinal household resilience data.

Acknowledgements

We are grateful to the Center for Climate Risk and Opportunity Management in Southeast Asia and Pacific (CCROM-SEAP), Bogor Agricultural University, and the Environmental Agency (DLH) of Jakarta for their collaboration and unwavering support in this research. Their essential role in providing data, performing analyses, and sharing profound insights has been vital to the progress of this study.

This research was supported by the Directorate General of Research and Development, Ministry of Higher Education, Science, and Technology, under the Research Program Implementation Contract for Fiscal Year 2025, No. 006/C3/DT.05.00/PL/2025.

Author Contributions

Conceptualization: Sundari, M., Sadik, K., Wigena, A. H., Fitrianto, A., Boer, R.; **methodology**: Sundari, M., Sadik, K., Wigena, A. H., Fitrianto, A., Boer; **investigation**: Sundari, M., Sadik, K., Wigena, A. H., Boer, R & Zulkarnain; **writing—original draft preparation**: Sundari, M., Sadik, K., Wigena, A. H., Boer, R., Zulkarnain; **writing—review and editing**: Sundari, M., Sadik, K., Wigena, A. H., Fitrianto, A., Boer, R., Zulkarnain; **visualization**: Sundari, M., Sadik, K., Wigena, A. H., Fitrianto, A., Boer, R., Zulkarnain. All authors have read and agreed to the published version of the manuscript.

All authors have read and agreed to the published version of the manuscript.

Conflict of interest

There are no conflicts to declare.

Funding

This research was supported by the Directorate General of Research and Development, Ministry of Higher Education, Science, and Technology, under the Research Program Implementation Contract for Fiscal Year 2025, No. 006/C3/DT.05.00/PL/2025.

References

Abidin, H. Z., Andreas, H., Gumilar, I., Fukuda, Y., Pohan, Y. E., & Deguchi, T. (2011). Land subsidence of Jakarta (Indonesia) and its relation with urban development. *Natural Hazards,* 59(3), 1753–1771.

Adger, W. N. (2000). Social and ecological resilience: are they related? *Progress in Human Geography,* 24(3), 347–364.

Albore, A., Tesfay, G., Zenebe, A., & Abadi, N. (2025). Livelihood resilience capacity and its determinants of Lowland Smallholder farmers to climate change-induced hazards in Wolaita Zone, Southern Ethiopia. *Sustainable Futures,* 10, 101370.

Bappeda Jakarta. (2018). *RPJMD DKI Jakarta 2017–2022e. Pemerintah Provinsi DKI Jakarta.* Retrieved From https://bappeda.jakarta.go.id/rpjmd/

Bertilsson, L., Wiklund, K., de Moura Tebaldi, I., Rezende, O. M., Veról, A. P., & Miguez, M. G. (2019). Urban flood resilience–A multi-criteria index to integrate flood resilience into urban planning. *Journal of Hydrology,* 573, 970–982.

Boer, R., Dasanto, B. D., Wijayanti, P., Jadmiko, S. D., Rafuddin, A., Anggraeni, L., & Hidayati, R. (2022). *Kajian Dampak Perubahan Iklim terhadap Lingkungan, Sosial, Ekonomi dan Kesehatan di Provinsi DKI Jakarta*. Retrieved From https://lingkunganhidup.jakarta.go.id/publikasi/aksi-api

Bott, L. M., Schöne, T., Illigner, J., Haghighi, M. H., Gisevius, K., & Braun, B. (2021). Land subsidence in Jakarta and Semarang Bay–The relationship between physical processes, risk perception, and household adaptation. *Ocean & Coastal Management,* 211, 105775. doi: 10.1016/j.ocecoaman.2021.105775

BPBD. (2021). *Infografis Kejadian Bencana Provinsi DKI Jakarta Tahun 2021.* Retrieved From https://bpbd.jakarta.go.id/infografis/30/hasil-rekapitulasi-kejadian-bencana-yang-ada-di-dki-jakarta-pada-tahun

BPS Jakarta, B. P. S. J. (2022). *DKI Jakarta dalam Angka 2022.* Retrieved From https://jakarta.bps.go.id

Chavent, M., Kuentz, V., Labenne, A., & Saracco, J. (2022). Multivariate analysis of mixed data. The R Package PCAmixdata. *Electronic Journal of Applied Statistical Analysis,* 15(3).

Cutter, S. L., Barnes, L., Berry, M., Burton, C., Evans, E., Tate, E., & Webb, J. (2008). A place-based model for understanding community resilience to natural disasters. *Global Environmental Change,* 18(4), 598–606.

Dinas Lingkungan Hidup Provinsi DKI Jakarta. (2021). Pelaksanaan Adaptasi dalam Rangka Memperkuat Ketahanan Iklim Provinsi DKI Jakarta.

Fajardo-Gonzalez, J., Lovell, C. A. K., Lovell, J., & Edmonds, H. (2025). Measuring climate risks: A new multidimensional index for global vulnerability and resilience. *Environmental Development,* 101227.

Ferrario, F., Mourato, J. M., Rodrigues, M. S., & Dias, L. F. (2024). Evaluating Nature-based Solutions as urban resilience and climate adaptation tools: A meta-analysis of their benefits on heatwaves and floods. *Science of The Total Environment,* 950, 175179. doi: 10.1016/j.scitotenv.2024.175179

Filzmoser, P., & Gregorich, M. (2020). Multivariate oOutlier dDetection in aApplied dData aAnalysis: Global, lLocal, cCompositional and cCellwise oOutliers. *Mathematical Geosciences,* 52(8), 1049–1066. doi: 10.1007/s11004-020-09861-6

Fotheringham, A., Brunsdon, C., & Charlton, M. (2002). Geographically Weighted Regression: The Analysis of Spatially Varying Relationships. *John Wiley & Sons,* 13.

Gollini, I., Lu, B., Charlton, M., Brunsdon, C., & Harris, P. (2015). GWmodel: An R Package for Exploring Spatial Heterogeneity Using Geographically Weighted Models. *Journal of Statistical Software,* 63(17 SE-Articles), 1–50. doi: 10.18637/jss.v063.i17

Green, B. (2017). The Method of Successive Intervals: A Sourcebook for Behavioral Scientists. *In Scaling: A Sourcebook for Behavioral Scientists*, 122–128. doi: 10.4324/9781315128948-13

Harintaka, H., Suhadha, A. G., Syetiawan, A., Ardha, M., & Rarasati, A. (2024). Current land subsidence in Jakarta: a multi-track SBAS InSAR analysis during 2017–2022 using C-band SAR data. *Geocarto International,* 39(1), 2364726.

Harris, P., Brunsdon, C., & Charlton, M. (2011). Geographically weighted principal components analysis. *International Journal of Geographical Information Science,* 25(10), 1717–1736.

Harris, P., Brunsdon, C., & Charlton, M. (2012). *Multivariate spatial outlier detection: a comparison of techniques. geoENV 2012.* Valencia, Spain.

Harris, P., Brunsdon, C., Charlton, M., Juggins, S., & Clarke, A. (2014). Multivariate spatial outlier detection using robust geographically weighted methods. *Mathematical Geosciences,* 46, 1–31.

Howe, L. D., Hargreaves, J. R., & Huttly, S. R. A. (2008). Issues in the construction of wealth indices for the measurement of socio-economic position in low-income countries. *Emerging Themes in Epidemiology,* 5(1), 3.

Hubert, M., & Rousseeuw, P. J. (2005). ROBPCA: A nNew aApproach to rRobust pPrincipal cComponent aAnalysis. *Technometrics,* 47(1), 64–79.

Hubert, M., Debruyne, M., & Rousseeuw, P. J. (2018). Minimum covariance determinant and extensions. *WIREs Comput. Stat.,* 10(3), 1421. doi: 10.1002/wics.1421

IPCC, I. P. on C. C. (2014). *Summary for policymakers. In: Climate Change 2014: Impacts, Adaptation, and Vulnerability. Part A: Global and Sectoral Aspects. Contribution of Working Group II to the Fifth Assessment Report of the Intergovernmental Panel on Climate Change. In Cambridge University Press.* Retrieved From https://doi.org/10.1017/cbo9780511976988.002

IPCC. (2022). Summary for Policymakers. In B. Pörtner, H.-O.; Roberts, D. C.; Poloczanska, E. S.; Mintenbeck, K.; Tignor, M.; Alegría, A.; Craig, M.; Langsdorf, S.; Löschke, S.; Möller, V.; Okem, A.; Rama (Ed.), Climate Change 2022: Impacts, Adaptation and Vulnerability. *Contribution of Working Group II to the Sixth Assessment Report of the Intergovernmental Panel on Climate Change,* 3–33. doi: 10.1017/9781009325844.001

Johnson, R. A., & Wichern, D. W. (2019). *Applied Multivariate Statistical Analysis. Pearson*. Retrieved From https://books.google.co.id/books?id=QBqlswEACAAJ

Jolliffe, I. T. (2002). *Principal component analysis, 2nd edn New York*. NY: Springer.[Google Scholar].

Jolliffe, I. T., & Cadima, J. (2016). Principal component analysis: a review and recent developments. Philosophical Transactions. *Series A, Mathematical, Physical, and Engineering Sciences,* 374(2065), 20150202. doi: 10.1098/rsta.2015.0202

Lee, H., Calvin, K., Dasgupta, D., Krinner, G., Mukherji, A., Thorne, P., Trisos, C., Romero, J., Aldunce, P., & Barret, K. (2023). IPCC, 2023: Climate change 2023: Synthesis report, summary for policymakers. Contribution of working groups i, II and III to the sixth assessment report of the intergovernmental panel on climate change [core writing team, h. Lee and j. Romero (eds.)]. IPC.

Li, C., Jin, B., & Wu, Y. (2024). Outlier detection via a minimum ridge covariance determinant estimator. *Statistica Sinica,* 34(4), 1923–1950. doi: 10.5705/ss.202022.0142

Lu, B., Harris, P., Charlton, M., & Brunsdon, C. (2014). The GWmodel R package: further topics for exploring spatial heterogeneity using geographically weighted models. *Geo-Spatial Information Science,* 17(2), 85–101.

Lu, B., Hu, Y., Yang, D., Liu, Y., Ou, G., Harris, P., Brunsdon, C., Comber, A., & Dong, G. (2025). GWmodelS: a standalone software to train geographically weighted models. *Geo-Spatial Information Science,* 28(2), 648–670. doi: 10.1080/10095020.2024.2343011

Mafi-Gholami, D., Frazier, T. G., Heydari, M., Danekar, A., & Nouri-kamari, A. (2026). A socio-ecological resilience index (SERI) framework for multi-hazard exposure: Insights from the Persian Gulf and Gulf of Oman. *Ocean & Coastal Management,* 272, 108011.

Maronna, R. A., Martin, R. D., Yohai, V. J., & Salibián-Barrera, M. (2019). *Robust statistics: theory and methods (with R) (2nd ed.).* John Wiley & Sons.

McPhearson, T., Cook, E. M., Berbés-Blázquez, M., Cheng, C., Grimm, N. B., Andersson, E., Barbosa, O., Chandler, D. G., Chang, H., Chester, M. V, Childers, D. L., Elser, S. R., Frantzeskaki, N., Grabowski, Z., Groffman, P., Hale, R. L., Iwaniec, D. M., Kabisch, N., Kennedy, C., … Troxler, T. G. (2022). A social-ecological-technological systems framework for urban ecosystem services. *One Earth,* 5(5), 505–518. doi: 10.1016/j.oneear.2022.04.007

Meerow, S., Newell, J. P., & Stults, M. (2016). Defining urban resilience: A review. *Landscape 748 and Urban Planning,* 147, 38–49.

Mosisa, G., Bedadi, B., Dale, G., & Abate, N. T. (2025). Nature-based solutions for urban climate resilience: implementation, contribution, and effectiveness. *Nature-Based Solutions,* 8, 100245. doi: 10.1016/j.nbsj.2025.100245

Norris, F. H., Stevens, S. P., Pfefferbaum, B., Wyche, K. F., & Pfefferbaum, R. L. (2008). Community resilience as a metaphor, theory, set of capacities, and strategy for disaster readiness. *American Journal of Community Psychology*, 41(1), 127–150.

Pagès, J. (2014). *Multiple factor analysis by example using R.* CRC Press.

Pécsinger, J., Macher, G. Z., Bódizs, D., Sipos, D., & Pestiné Rácz, É. V. (2025). Assessing the Urban Climate Resilience of Cities in Hungary Using an Index-based Approach. *Journal of Sustainable Development of Energy, Water and Environment Systems,* 13(3), 1–22.

Polydoropoulou, A., Velegrakis, A., Papaioannou, G., Karakikes, I., Bouhouras, E., Thanopoulou, H., Chatzistratis, D., Monioudi, I., Moschopoulos, K., & Chatzipavlis, A. (2025). A composite port resilience index focused on climate-related hazards: Results from Greek ports' living-labs. *Maritime Transport Research,* 9, 100136.

Rousseeuw, P. J. (1984). Least mMedian of sSquares rRegression. *Journal of the American Statistical Association,* 79(388), 871–880. doi: 10.2307/2288718

Rousseeuw, P. J., & Driessen, K. Van. (1999). A fast algorithm for the minimum covariance determinant estimator. *Technometrics,* 41(3), 212–223.

Roy, S., Basu, A., & Ghosh, A. (2024). Robust principal component analysis using density power divergence. *Journal of Machine Learning Research,* 25(324), 1–40

Schipper, E. L. F., Revi, A., Preston, B. L., Carr, E. R., Eriksen, S. H., Fernandez-Carril, L. R., Glavovic, B., Hilmi, N. J. M., Ley, D., Mukerji, R., Araujo, M. de, R, P., SK, R., & PK, S. (2022). *Climate resilient development pathways. In Climate Change 2022: Impacts, Adaptation, and Vulnerability. Contribution of Working Group II to the Sixth Assessment Report of the Intergovernmental Panel on Climate Change (pp. 2655–2807). Cambridge University Press.* Retrieved From https://doi.org/10.1017/9781009325844.027

Sharifi, A. (2023). Resilience of urban social-ecological-technological systems (SETS): A review. *Sustainable Cities and Society*, 99, 104910.

Singh, R., Maiti, S., Garai, S., Bhakat, M., Jha, S. K., Dixit, A. K., & Aggarwal, A. (2025). Assessment of climate resilience index: Insight from Murrah buffalo-based livestock production system of Western India. *Agricultural Systems,* 228, 104390.

Suárez, M., Benayas, J., Justel, A., Sisto, R., Montes, C., & Sanz-Casado, E. (2024). A holistic index-based framework to assess urban resilience: Application to the Madrid Region, Spain. *Ecological Indicators,* 166, 112293. doi: 10.1016/j.ecolind.2024.112293

Subiyanto, A., Boer, R., Aldrian, E., & Kinseng, R. (2020). Climate Resilience: Concepts, Theory and Methods of Measuring. *EnvironmentAsia*, 13(1).

Sundari, M., Sadik, K., Wigena, A. H., Fitrianto, A., & Boer, R. (2026). Household Climate Resilience Index and Its Determinants: An Empirical Study in DKI Jakarta. *Jurnal Pengelolaan Sumberdaya Alam Dan Lingkungan (Journal of Natural Resources and Environmental Management),* 16(2)162.

Townend, I., French, J., & Nicholls, R. (2024). Framing resilience to manage complex environmental systems. *One Earth,* 7(11), 1941–1952. doi: 10.1016/j.oneear.2024.09.008

Tsutsumida, N., Murakami, D., Yoshida, T., Nakaya, T., Lu, B., Harris, P., & Comber, A. (2022). A Comparison of Geographically Weighted Principal Components Analysis Methodologies. In T. Ishikawa, S. I. Fabrikant, & S. Winter (Eds.), *15th International Conference on Spatial Information Theory (COSIT 2022),* 240(21), 1-21. doi: 10.4230/LIPIcs.COSIT.2022.21

Upendra, S., Abbaiah, D., & Balasiddamuni, D. (2023). Multicollinearity in Multiple Linear Regression: Detection, Consequences, and Remedies. *International Journal for Research in Applied Science and Engineering Technology,* 11, 1047–1061. doi: 10.22214/ijraset.2023.55786

Vyas, S., & Kumaranayake, L. (2006). Constructing socio-economic status indices: how to use principal components analysis. *Health Policy and Planning,* 21(6), 459–468.